

2 **The protonmotive force and respiratory control:**

3 **Building blocks of mitochondrial physiology**

4 **Part 1.**

5 http://www.mitoeagle.org/index.php/MitoEAGLE_preprint_2017-09-21

6 Preprint version 10 (2017-10-15)

7
8 **MitoEAGLE Network**

9 Corresponding author: Gnaiger E

10 Contributing co-authors

11 Ahn B, Alves MG, Amati F, Åsander Frostner E, Bailey DM, Battino M, Beard DA, Ben-
12 Shachar D, Bishop D, Breton S, Brown GC, Brown RA, Buettner GR, Carvalho E,
13 Cervinkova Z, Chicco AJ, Coen PM, Collins JL, Crisóstomo L, Davis MS, Dias T, Distefano
14 G, Doerrier C, Ehinger J, Elmer E, Fell DA, Ferko M, Ferreira JCB, Filipovska A, Fisher J,
15 Garcia-Roves PM, Garcia-Souza LF, Genova ML, Gonzalo H, Goodpaster BH, Gorr TA, Han
16 J, Harrison DK, Hellgren KT, Hernansanz P, Holland O, Hoppel CL, Iglesias-Gonzalez J,
17 Irving BA, Iyer S, Jansen-Dürr P, Jespersen NR, Jha RK, Kaambre T, Kane DA, Kappler L,
18 Keijer J, Komlodi T, Kopitar-Jerala N, Krako Jakovljevic N, Kuang J, Labieniec-Watala M,
19 Lai N, Laner V, Lee HK, Lemieux H, Lerfall J, Lucchinetti E, MacMillan-Crow LA,
20 Makrecka-Kuka M, Meszaros AT, Moiso N, Molina AJA, Montaigne D, Moore AL, Murray
21 AJ, Newsom S, Nozickova K, O'Gorman D, Oliveira PF, Oliveira PJ, Orynbayeva Z, Pak YK,
22 Palmeira CM, Patel HH, Pesta D, Petit PX, Pichaud N, Pirkmajer S, Porter RK, Pranger F,
23 Prochownik EV, Radenkovic F, Reboredo P, Renner-Sattler K, Robinson MM, Rohlena J,
24 Røsland GV, Rossiter HB, Salvadego D, Scatena R, Schartner M, Scheibye-Knudsen M,
25 Schilling JM, Schlattner U, Schoenfeld P, Scott GR, Singer D, Sobotka O, Spinazzi M, Stier
26 A, Stocker R, Sumbalova Z, Suravajhala P, Tanaka M, Tandler B, Tepp K, Tomar D,

27 Towheed A, Trivigno C, Tronstad KJ, Trougakos IP, Tyrrell DJ, Velika B, Vendelin M,
28 Vercesi AE, Victor VM, Ward ML, Watala C, Wei YH, Wieckowski MR, Wohlwend M,
29 Wolff J, Wuest RCI, Zaugg K, Zaugg M, Zorzano A

30

31 Supporting co-authors:

32 Arandarčikaitė O, Bakker BM, Bernardi P, Boetker HE, Borsheim E, Borutaitė V, Bouitbir J,
33 Calabria E, Calbet JA, Chaurasia B, Clementi E, Coker RH, Collin A, Das AM, De Palma C,
34 Dubouchaud H, Duchon MR, Durham WJ, Dyrstad SE, Engin AB, Fornaro M, Gan Z, Garlid
35 KD, Garten A, Gourlay CW, Granata C, Haas CB, Haavik J, Haendeler J, Hand SC, Hepple
36 RT, Hickey AJ, Hoel F, Kainulainen H, Keppner G, Khamoui AV, Klingenspor M, Koopman
37 WJH, Kowaltowski AJ, Krajcova A, Lenaz G, Malik A, Markova M, Mazat JP, Menze MA,
38 Methner A, Muntané J, Muntean DM, Neuzil J, Oliveira MT, Pallotta ML, Parajuli N,
39 Pettersen IKN, Pulinilkunnil T, Ropelle ER, Salin K, Sandi C, Sazanov LA, Siewiera K,
40 Silber AM, Skolik R, Smenes BT, Soares FAA, Sokolova I, Sonkar VK, Stankova P,
41 Swerdlow RH, Szabo I, Trifunovic A, Thyfault JP, Tretter L, Vieyra A, Votion DM, Williams

42

C

43

44

Updates:

45

http://www.mitoeagle.org/index.php/MitoEAGLE_preprint_2017-09-21

46

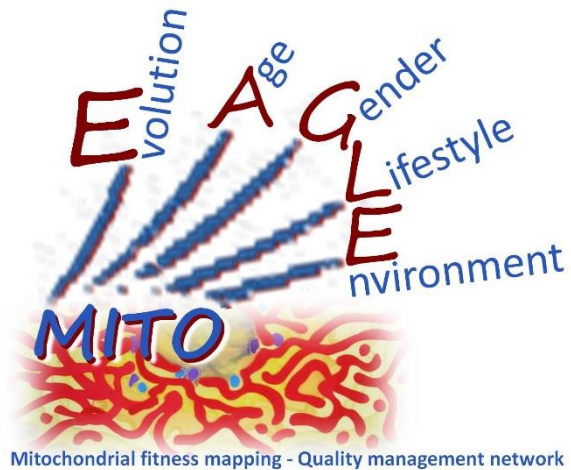
Correspondence: Gnaiger E

Department of Visceral, Transplant and Thoracic Surgery, D. Swarovski Research Laboratory, Medical University of Innsbruck, Innrain 66/4, A-6020 Innsbruck, Austria

Email: erich.gnaiger@i-med.ac.at

Tel: +43 512 566796, Fax: +43 512 566796 20

This manuscript on 'The protonmotive force and respiratory control' is a position statement in the frame of COST Action CA15203 MitoEAGLE. The list of co-authors evolved from MitoEAGLE Working Group Meetings and a **bottom-up** spirit of COST in phase 1: This is an open invitation to scientists and students to join as co-authors, to provide a balanced view on mitochondrial respiratory control, a fundamental introductory presentation of the concept of the protonmotive force, and a consensus statement on reporting data of mitochondrial respiration in terms of metabolic flows and fluxes. We plan a series of follow-up reports by the expanding MitoEAGLE Network, to increase the scope of recommendations on harmonization and facilitate global communication and collaboration.



Phase 2: MitoEAGLE preprint (Versions 01 – 10): We continue to invite comments and suggestions on the, particularly if you are an **early career investigator adding an open future-oriented perspective**, or an **established scientist providing a balanced historical basis**. Your critical input into the quality of the manuscript will be most welcome, improving our aims to be educational, general, consensus-oriented, and practically helpful for students working in mitochondrial respiratory physiology.

Phase 3 (2017-11-11): Manuscript submission to a preprint server, such as BioRxiv. We want to invite further opinion leaders: To join as a co-author, please feel free to focus on a particular section in terms of direct input and references, contributing to the scope of the manuscript from the perspective of your expertise. Your comments will be largely posted on the discussion page of the MitoEAGLE preprint website.

If you prefer to submit comments in the format of a referee's evaluation rather than a contribution as a co-author, I will be glad to distribute your views to the updated list of co-authors for a balanced response. We would ask for your consent on this open bottom-up policy.

Phase 4: We organize a MitoEAGLE session linked to our series of reports at the MiPconference Nov 2017 in Hradec Kralove in close association with the MiP society (where you hopefully will attend) and at EBEC 2018 in Budapest.

» http://www.mitoeagle.org/index.php/MiP2017_Hradec_Kralove_CZ

I thank you in advance for your feedback.

With best wishes,

Erich Gnaiger

Chair Mitochondrial Physiology Society - <http://www.mitophysiology.org>

Chair COST Action MitoEAGLE - <http://www.mitoeagle.org>

Medical University of Innsbruck, Austria

97	Contents
98	1. Introduction
99	2. Respiratory coupling states in mitochondrial preparations
100	Mitochondrial preparations
101	2.1. <i>Three coupling states of mitochondrial preparations and residual oxygen consumption</i>
102	Coupling control states and respiratory capacities
103	Kinetic control
104	Phosphorylation, P _o
105	LEAK, OXPHOS, ET, ROX
106	2.2. <i>Coupling states and respiratory rates</i>
107	2.3. <i>Classical terminology for isolated mitochondria</i>
108	States 1-5
109	3. The protonmotive force and proton flux
110	3.1. <i>Electric and chemical partial forces versus electrical and chemical units</i>
111	Faraday constant
112	Electrical part of the protonmotive force
113	Chemical part of the protonmotive force
114	3.2. <i>Definitions</i>
115	Control and regulation
116	Respiratory control and response
117	Respiratory coupling control
118	Pathway control states
119	The steady-state
120	3.3. <i>Forces and fluxes in physics and irreversible thermodynamics</i>
121	Vectorial and scalar forces, and fluxes
122	Coupling
123	Coupled versus bound processes
124	4. Normalization: fluxes and flows
125	4.1. <i>Flux per chamber volume</i>
126	4.2. <i>System-specific and sample-specific normalization</i>
127	Extensive quantities
128	Size-specific quantities
129	Molar quantities
130	Flow per system, I
131	Size-specific flux, J
132	Sample concentration, C_{mX}
133	Mass-specific flux, J_{mX,O_2}
134	Number concentration, C_{NX}
135	Flow per sample entity, I_{X,O_2}
136	4.3. <i>Normalization for mitochondrial content</i>
137	Mitochondrial concentration, C_{mte} , and mitochondrial markers
138	Mitochondria-specific flux, J_{mte,O_2}
139	4.4. <i>Conversion: units and normalization</i>
140	4.5. <i>Conversion: oxygen, proton and ATP flux</i>
141	5. Conclusions
142	6. References
143	

144 **Abstract**

145 Clarity of concept and consistency of nomenclature are key trademarks of a research field.
146 These trademarks facilitate effective transdisciplinary communication, education, and
147 ultimately further discovery. As the knowledge base and importance of mitochondrial
148 physiology to human health expand, the necessity for harmonizing nomenclature concerning
149 mitochondrial respiratory states and rates has become increasingly apparent. Peter Mitchell's
150 concept of the protonmotive force establishes the links between electrical and chemical
151 components of energy transformation and coupling in oxidative phosphorylation. This unifying
152 concept provides the framework for developing a consistent nomenclature for mitochondrial
153 physiology and bioenergetics. Herein, we follow IUPAC guidelines on general terms of
154 physical chemistry, extended by the concepts of open systems and irreversible thermodynamics.
155 We align the nomenclature of classical bioenergetics on respiratory states with a concept-driven
156 constructive terminology to address the meaning of each respiratory state. Furthermore, we
157 suggest uniform standards for the evaluation of respiratory states that will ultimately support
158 the development of databases of mitochondrial respiratory function in species, tissues and cells
159 studied under diverse physiological and experimental conditions. In this position statement, in
160 the frame of COST Action CA15203 MitoEAGLE, we endeavour to provide a balanced view
161 on mitochondrial respiratory control, a fundamental introductory presentation of the concept of
162 the protonmotive force, and a critical discussion on reporting data of mitochondrial respiration
163 in terms of metabolic flows and fluxes.

164

165 *Keywords:* Mitochondrial respiratory control, coupling control, mitochondrial
166 preparations, protonmotive force, chemiosmotic theory, oxidative phosphorylation, OXPHOS,
167 efficiency, electron transfer, ET; proton leak, LEAK, residual oxygen consumption, ROX, State
168 2, State 3, State 4, normalization, flow, flux

169

170

171 **Box 1:**

172

173 **In brief:**174 **mitochondria**175 **and Bioblasts**

- * Does the public expect biologists to understand Darwin's theory of evolution?
- * Do students expect that researchers of bioenergetics can explain Mitchell's theory of chemiosmotic energy transformation?

176 **Mitochondria** were described for the first time in 1857 by Rudolph Albert von Kölliker as

177 granular structures or 'sarkosomes'. In 1886 Richard Altman called them 'bioblasts' (published

178 1894). The word 'mitochondrium' (Greek mitos: thread; chondros: granule) was introduced by

179 Carl Benda (1898). Mitochondria are the oxygen consuming electrochemical generators which

180 evolved from endosymbiotic bacteria (Margulis 1970; Lane 2005). The bioblasts of Richard

181 Altmann (1894) included, not only the mitochondria as presently defined, but also symbiotic

182 and free-living bacteria.

183 We now recognize mitochondria as dynamic organelles with a double membrane that are

184 contained within eukaryotic cells. The inner mitochondrial membrane shows dynamic tubular

185 and disk-shaped cristae that separate the mitochondrial matrix, *i.e.* the internal mitochondrial

186 compartment, and the intermembrane space; the latter being enclosed by the outer

187 mitochondrial membrane. Mitochondria are the structural and functional elemental units of cell

188 respiration, where cell respiration is defined as the consumption of oxygen coupled to

189 electrochemical proton translocation across the inner mitochondrial membrane. In the process

190 of oxidative phosphorylation (OXPHOS), the reduction of O₂ is electrochemically coupled to

191 the transformation of energy in the form of adenosine triphosphate (ATP; Mitchell 2011). These

192 powerhouses of the cell contain the machinery of the OXPHOS pathway, including

193 transmembrane respiratory complexes (*i.e.* proton pumps with FMN, Fe-S and cytochrome *b*,194 *c*, *aa*₃ redox systems); alternative dehydrogenases and oxidases; the coenzyme ubiquinone

195 (coenzyme Q); ATP synthase; the enzymes of the tricarboxylic acid cycle and the fatty acid

196 oxidation enzymes; transporters of ions, metabolites and co-factors; and mitochondrial kinases

197 related to energy transfer pathways. The mitochondrial proteome comprises over 1,200 proteins

198 (MITOCARTA), mostly encoded by nuclear DNA (nDNA), with a variety of functions, many
199 of which are relatively well known (*e.g.* apoptosis-regulating proteins), while others are still
200 under investigation, or need to be identified (*e.g.* alanine transporter).

201 Mitochondria typically maintain several copies of their own genome (hundred to
202 thousands per cell; Cummins 1998), which is almost exclusively maternally inherited (White *et*
203 *al.* 2008) and known as mitochondrial DNA (mtDNA). One exception to strictly maternal
204 inheritance in animals is found in bivalves (Breton *et al.* 2007). mtDNA is 16.5 Kb in length,
205 contains 13 protein-coding genes for subunits of the transmembrane respiratory Complexes CI,
206 CIII, CIV and ATP synthase, and also encodes 22 tRNAs and the mitochondrial 16S and 12S
207 rRNA. The mitochondrial genome is both regulated and supplemented by nuclear-encoded
208 mitochondrial targeted proteins. Evidence has accumulated that additional gene content is
209 encoded in the mitochondrial genome, *e.g.* microRNAs, piRNA, smithRNAs, repeat associated
210 RNA, and even additional proteins (Duarte *et al.* 2014; Lee *et al.* 2015; Cobb *et al.* 2016).

211 The inner mitochondrial membrane contains the non-bilayer phospholipid cardiolipin,
212 which is not present in any other eukaryotic cellular membrane. Cardiolipin promotes the
213 formation of respiratory supercomplexes, which are supramolecular assemblies based upon
214 specific, though dynamic, interactions between individual respiratory complexes (Greggio *et*
215 *al.* 2017; Lenaz *et al.* 2017). Membrane fluidity is an important parameter influencing
216 functional properties of proteins incorporated in the membranes (Waczulikova *et al.* 2007).
217 There is a constant crosstalk between mitochondria and the other cellular components,
218 maintaining cellular mitostasis through regulation at both the transcriptional and post-
219 translational level, and through cell signalling including proteostatic (*e.g.* the ubiquitin-
220 proteasome and autophagy-lysosome pathways) and genome stability modules throughout the
221 cell cycle or even cell death, contributing to homeostatic regulation in response to varying
222 energy demands and stress (Quiros *et al.* 2016). In addition to mitochondrial movement along
223 the microtubules, mitochondrial morphology can change in response to the energy requirements

224 of the cell via processes known as fusion and fission, through which mitochondria can
225 communicate within a network, and in response to intracellular stress factors causing swelling
226 and ultimately permeability transition.

227 Mitochondrial dysfunction is associated with a wide variety of genetic and degenerative
228 diseases. Robust mitochondrial function is supported by physical exercise and caloric balance,
229 and is central for sustained metabolic health throughout life. Therefore, a better understanding
230 of mitochondrial physiology will improve our understanding of the etiology of disease, the
231 diagnostic repertoire of mitochondrial medicine, with a focus on protective medicine, lifestyle
232 and healthy aging.

233 Abbreviation: mt, as generally used in mtDNA. Mitochondrion is singular and
234 mitochondria is plural.

235 *‘For the physiologist, mitochondria afforded the first opportunity for an experimental*
236 *approach to structure-function relationships, in particular those involved in active transport,*
237 *vectorial metabolism, and metabolic control mechanisms on a subcellular level’ (Ernster and*
238 *Schatz 1981).*

239

240 **1. Introduction**

241 Mitochondria are the powerhouses of the cell with numerous physiological, molecular,
242 and genetic functions (**Box 1**). Every study of mitochondrial function and disease is faced with
243 **E**volution, **A**ge, **G**ender and sex, **L**ifestyle, and **E**nvironment (EAGLE) as essential background
244 conditions intrinsic to the individual patient or subject, cohort, species, tissue and to some extent
245 even cell line. As a large and highly coordinated group of laboratories and researchers, the
246 mission of the global MitoEAGLE Network is to generate the necessary scale, type, and quality
247 of consistent data sets and conditions to address this intrinsic complexity. Harmonization of
248 experimental protocols and implementation of a quality control and data management system
249 is required to interrelate results gathered across a spectrum of studies and to generate a

250 rigorously monitored database focused on mitochondrial respiratory function. In this way,
251 researchers within the same and across different disciplines will be positioned to compare their
252 findings to an agreed upon set of clearly defined and accepted international standards.

253 Reliability and comparability of quantitative results depend on the accuracy of
254 measurements under strictly-defined conditions. A conceptually clearly-defined framework is
255 also required to warrant meaningful interpretation and comparability of experimental outcomes
256 carried out by research groups at different institutes. With an emphasis on quality of research,
257 collected data can be useful far beyond the specific question of a specific experiment. Thus
258 enabling meta-analytic studies is the most economic way of providing robust answers to
259 biological questions (Cooper *et al.* 2009). Vague or ambiguous jargon can lead to confusion
260 and may relegate valuable signals to wasteful noise. For this reason, measured values must be
261 expressed in standardized units for each parameter used to define mitochondrial respiratory
262 function. Standardization of nomenclature and technical terms is essential to improve the
263 awareness of the intricate meaning of a divergent scientific vocabulary. The focus on coupling
264 states, the protonmotive force and fluxes through metabolic pathways of aerobic energy
265 transformation in mitochondrial preparations is a first step in the attempt to generate a
266 harmonized and conceptually-oriented nomenclature in bioenergetics and mitochondrial
267 physiology. Coupling states of intact cells and respiratory control by fuel substrates and specific
268 inhibitors of respiratory enzymes will be reviewed in subsequent communications.

269

270 **2. Respiratory coupling states in mitochondrial preparations**

271 *‘Every professional group develops its own technical jargon for talking about*
272 *matters of critical concern ... People who know a word can share that idea with*
273 *other members of their group, and a shared vocabulary is part of the glue that holds*
274 *people together and allows them to create a shared culture’ (Miller 1991).*

275

276 **Mitochondrial preparations** are defined as either isolated mitochondria, or tissue and
277 cellular preparations in which the barrier function of the plasma membrane is disrupted. The
278 plasma membrane separates the cytosol, nucleus, and organelles (the intracellular
279 compartment) from the environment of the cell. The plasma membrane consists of a lipid
280 bilayer, embedded proteins, and attached organic molecules that collectively control the
281 selective permeability of ions, organic molecules, and particles across the cell boundary. The
282 intact plasma membrane, therefore, prevents the passage of many water-soluble mitochondrial
283 substrates, such as succinate or adenosine diphosphate (ADP), that are required for the analysis
284 of respiratory capacity at kinetically-saturating concentrations, thus limiting the scope of
285 investigations into mitochondrial respiratory function in intact cells. The cholesterol content of
286 the plasma membrane is high compared to mitochondrial membranes. Therefore, mild
287 detergents, such as digitonin and saponin, can be applied to selectively permeabilize the plasma
288 membrane by interaction with cholesterol and allow free exchange of cytosolic components
289 with ions and organic molecules of the immediate cell environment, while maintaining the
290 integrity and localization of organelles, cytoskeleton, and the nucleus. Application of optimum
291 concentrations of these mild detergents leads to the complete loss of cell viability, tested by
292 nuclear staining, while mitochondrial function remains unaffected, as shown by an unaltered
293 respiration rate of mitochondria after the addition of such low concentrations of digitonin and
294 saponin. In addition to mechanical permeabilization during homogenization of fresh tissue,
295 saponin may be applied to ensure permeabilization of all cells. Crude homogenate and cells
296 permeabilized in the respiration chamber contain all components of the cell at highly diluted
297 concentrations. All mitochondria are retained in chemically-permeabilized mitochondrial
298 preparations and crude tissue homogenates. In the preparation of isolated mitochondria, the
299 cells or tissues are homogenized, and the mitochondria are separated from other cell fractions
300 and purified by differential centrifugation, entailing the loss of a significant fraction of

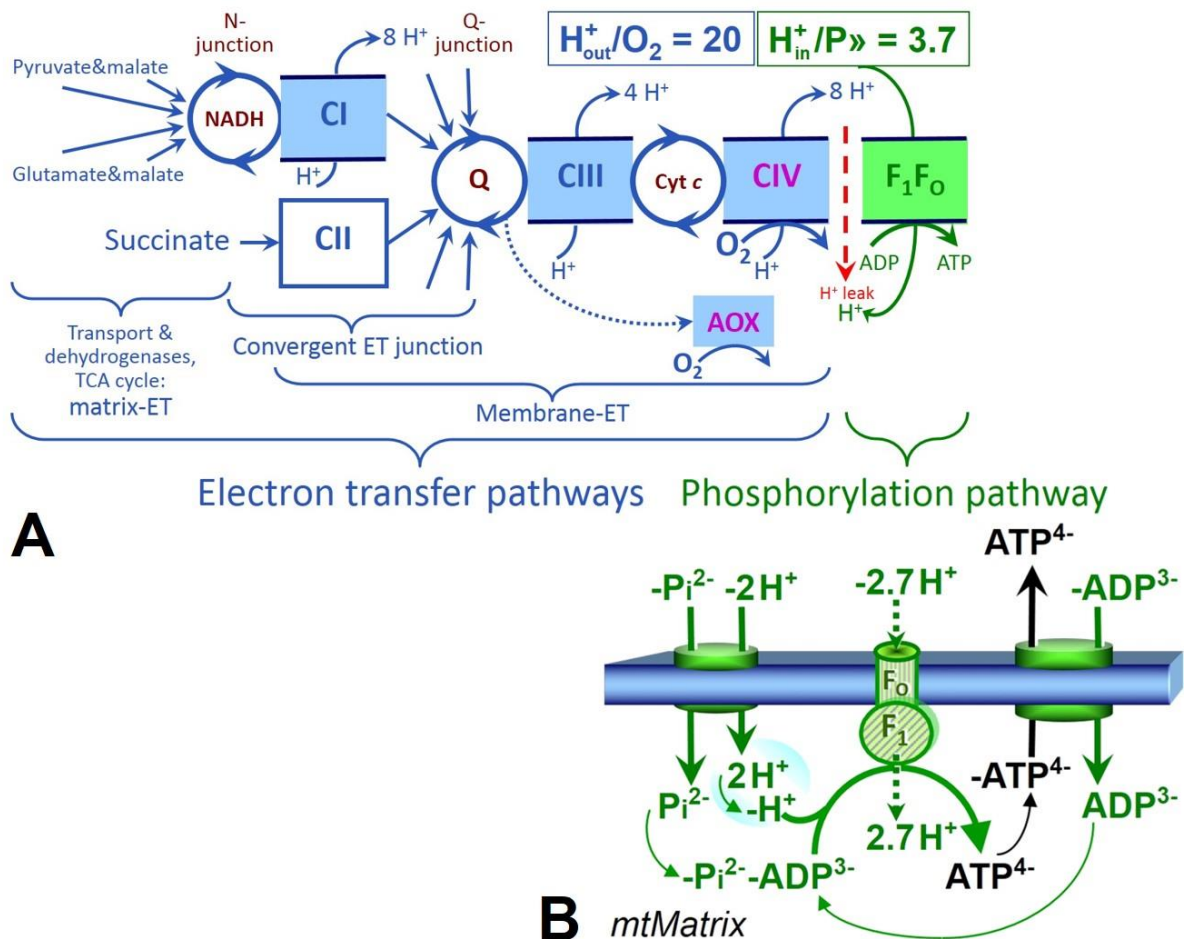
301 mitochondria. The term mitochondrial preparation does not include further fractionation of
302 mitochondrial components, as well as submitochondrial particles.

303

304 *2.1. Three coupling states of mitochondrial preparations and residual oxygen consumption*

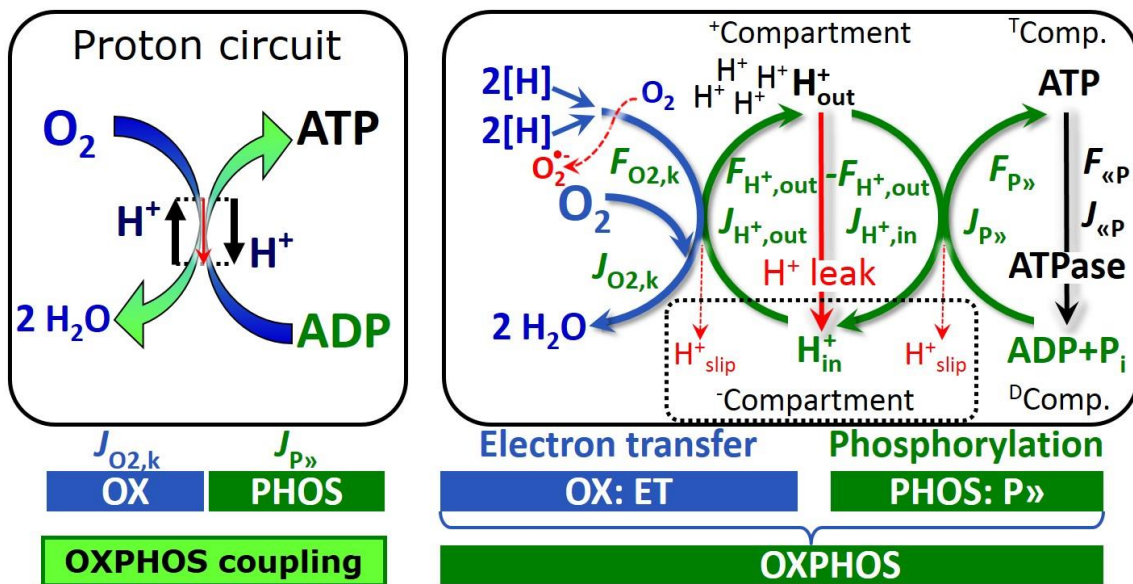
305 **Respiratory capacities in coupling control states:** To extend the classical nomenclature
306 on mitochondrial coupling states (Section 2.4) by a concept-driven terminology that
307 incorporates explicit information on the nature of the respiratory states, the terminology must
308 be general and not restricted to any particular experimental protocol or mitochondrial
309 preparation (Gnaiger 2009). We focus primarily on the conceptual ‘why’, along with
310 clarification of the experimental ‘how’. In the following section, the concept-driven
311 terminology is explained and coupling states are defined. We define respiratory capacities,
312 comparable to channel capacity in information theory (Schneider 2006), as the upper bound of
313 the rate of respiration measured in defined coupling and pathway control states of mitochondrial
314 preparations. To provide a diagnostic reference for respiratory capacities of core energy
315 metabolism, the capacity of *oxidative phosphorylation*, OXPHOS, is measured at kinetically-
316 saturating concentrations of ADP and inorganic phosphate, P_i. The *oxidative* capacity of the
317 electron transfer-pathway, ET-pathway, reveals the limitation of OXPHOS capacity mediated
318 by the *phosphorylation* pathway. The ET and phosphorylation pathways comprise coupled
319 segments of the OXPHOS pathway. ET capacity is measured as noncoupled respiration by
320 application of *external uncouplers*. The contribution of *intrinsically uncoupled* oxygen
321 consumption is most easily studied by not stimulating or arresting phosphorylation, when
322 oxygen consumption compensates mainly for the proton leak; the corresponding states are
323 collectively classified as LEAK states (**Table 1**). Fuel substrates and ET inhibitors are kept
324 constant, *i.e.* maintaining a defined ET-pathway state, while (1) adding ADP or P_i, (2) inhibiting
325 the phosphorylation pathway, and (3) performing uncoupler titrations to induce different
326 coupling states (**Fig. 1**).

327 **Kinetic control:** Coupling control states are established in the study of mitochondrial
 328 preparations to obtain reference values for various output variables. Physiological conditions *in*
 329 *vivo* may deviate substantially from these experimentally obtained states. Since kinetically-
 330 saturating concentrations, *e.g.* of ADP or oxygen, may not apply to physiological intracellular
 331 conditions, relevant information is obtained in studies of kinetic responses to conditions
 332 intermediate between the LEAK state at zero [ADP] and the OXPHOS state at saturating
 333 [ADP], or of respiratory capacities in the range between kinetically-saturating [O₂] and anoxia
 334 (Gnaiger 2001).



335
 336 **Fig. 1. The oxidative phosphorylation pathway, OXPHOS pathway.** (A) Electron transfer, ET,
 337 coupled to phosphorylation. Multiple convergent electron transfer pathways are shown from NADH and
 338 succinate; additional arrows indicate electron entry through electron transferring flavoprotein,
 339 glycerophosphate dehydrogenase, dihydro-otrate dehydrogenase, choline dehydrogenase, and
 340 sulfide-ubiquinone oxidoreductase. The branched pathway of oxygen consumption by alternative quinol

341 oxidase (AOX) is indicated by the dotted arrow. H^+_{out}/O_2 is the ratio of outward proton flux from the matrix
 342 space to catabolic O_2 flux in the NADH-linked pathway. $H^+_{in}/P\gg$ is the ratio of inward proton flux from the
 343 inter-membrane space to the flux of phosphorylation of ADP to ATP. Due to proton leak and slip these
 344 are not fixed stoichiometries. (B) Phosphorylation pathway catalyzed by the F_1F_0 ATP synthase,
 345 adenine nucleotide translocase, and inorganic phosphate transporter. The $H^+_{in}/P\gg$ stoichiometry is the
 346 sum of the coupling stoichiometry in the ATP synthase reaction (-2.7 H^+ from the intermembrane space,
 347 2.7 H^+ to the matrix) and the proton balance in the translocation of ADP^{2-} , ATP^{3-} and P_i^{2-} . See Eqs. 3
 348 and 4 for further explanation. Modified from (A) Lemieux *et al.* (2017) and (B) Gnaiger (2014).
 349



350
 351 **Fig. 2. The proton circuit and coupling in oxidative phosphorylation (OXPHOS).** Oxygen flux, $J_{O_2,k}$,
 352 through the catabolic electron transfer (ET) pathway k is coupled to flux through the phosphorylation
 353 pathway of ADP to ATP, $J_{P\gg}$, by the proton pumps of the ET-pathway, pushing the outward proton flux,
 354 $J_{H^+,out}$, and generating the output protonmotive force, $F_{H^+,out}$. ATP synthase is coupled to inward proton
 355 flux, $J_{H^+,in}$, to phosphorylate ADP with inorganic phosphate to ATP, driven by the input protonmotive
 356 force, $F_{H^+,in} = -F_{H^+,out}$. $2[H]$ indicates the reduced hydrogen equivalents of fuel substrates that provide
 357 the chemical input force, $F_{O_2,k}$ [kJ/mol O_2], of the catabolic reaction k with oxygen (Gibbs energy of
 358 reaction per mole O_2 consumed in reaction k), typically in the range of -460 to -480 kJ/mol. The output
 359 force is given by the phosphorylation potential difference (ADP phosphorylated to ATP), $F_{P\gg}$, which
 360 varies *in vivo* ranging from about 48 to 62 kJ/mol under physiological conditions. Fluxes, J_B , and forces,
 361 F_B , are expressed in either chemical units, [$mol \cdot s^{-1} \cdot m^{-3}$] and [$J \cdot mol^{-1}$] respectively, or electrical units,

362 $[\text{C}\cdot\text{s}^{-1}\cdot\text{m}^{-3}]$ and $[\text{J}\cdot\text{C}^{-1}]$ respectively, per volume, V $[\text{m}^3]$, of the system. The system defined by the
 363 boundaries shown as a full black line is not a black box, but is analysed as a compartmental system.
 364 The negative compartment (N-compartment, enclosed by the dotted line) is the matrix space, separated
 365 from the positive compartment (+Compartment) by the inner mitochondrial membrane. $\text{ADP}+\text{P}_i$ and ATP
 366 are the substrate- and product-compartments (scalar ADP and ATP compartments, $^{\text{D}}\text{Comp.}$ and
 367 $^{\text{T}}\text{Comp.}$), respectively. Chemical potentials of all substrates and products involved in the scalar reactions
 368 are measured in the +Compartment for calculation of the scalar forces $F_{\text{O}_2,k}$ and $F_{\text{P}\gg} = -F_{\ll\text{P}}$ (**Box 2**).
 369 Modified from Gnaiger (2014).

370

371 **Phosphorylation, $\text{P}\gg$:** *Phosphorylation* in the context of OXPHOS is defined as
 372 phosphorylation of ADP to ATP. On the other hand, the term phosphorylation is used generally
 373 in many different contexts, *e.g.* protein phosphorylation. This justifies consideration of a
 374 symbol more discriminating and specific than P as used in the P/O ratio (phosphate to atomic
 375 oxygen ratio; $\text{O} = 0.5 \text{O}_2$), where P indicates phosphorylation of ADP to ATP or GDP to GTP.
 376 We propose the symbol $\text{P}\gg$ for the endergonic direction of phosphorylation $\text{ADP}\rightarrow\text{ATP}$, and
 377 likewise the symbol $\ll\text{P}$ for the corresponding exergonic hydrolysis $\text{ATP}\rightarrow\text{ADP}$ (**Fig. 2; Box**
 378 **3**). ATP synthase is the proton pump of the phosphorylation pathway (**Fig. 1B**). $\text{P}\gg$ may also
 379 involve substrate-level phosphorylation as part of the tricarboxylic acid cycle (succinyl-CoA
 380 ligase) and phosphorylation of ADP catalyzed by phosphoenolpyruvate carboxykinase,
 381 adenylate kinase, creatine kinase, hexokinase and nucleoside diphosphate kinase (NDPK).
 382 Kinase cycles are involved in intracellular energy transfer and signal transduction for regulation
 383 of energy flux. In isolated mammalian mitochondria ATP production catalyzed by adenylate
 384 kinase, $2\text{ADP} \leftrightarrow \text{ATP} + \text{AMP}$, proceeds without fuel substrates in the presence of ADP
 385 (Komlódi and Tretter 2017). $J_{\text{P}\gg}/J_{\text{O}_2,k}$ ($\text{P}\gg/\text{O}_2$) is two times the 'P/O' ratio of classical
 386 bioenergetics. The effective $\text{P}\gg/\text{O}_2$ ratio is diminished by: (1) the proton leak across the inner
 387 mitochondrial membrane from low pH in the +Compartment to high pH in the negative
 388 compartment ($^{\text{C}}\text{Compartment}$); (2) cycling of other cations; (3) proton slip in the proton pumps

389 when a proton effectively is not pumped; and (4) electron leak in the univalent reduction of
 390 oxygen (O_2 ; dioxygen) to superoxide anion radical ($O_2^{\bullet-}$).

391

392 **Table 1. Coupling states and residual oxygen consumption in mitochondrial**
 393 **preparations in relation to respiration and phosphorylation rate, $J_{O_2,k}$ and $J_{P_{\gg}}$,**
 394 **and protonmotive force, $F_{H^+,out}$.** Coupling states are established at kinetically-
 395 saturating concentrations of fuel substrates and O_2 .

State	$J_{O_2,k}$	$J_{P_{\gg}}$	$F_{H^+,out}$	Inducing factors	Limiting factors
LEAK	L ; low proton leak-dependent respiration	0	max.	Proton leak, slip, and cation cycling	$J_{P_{\gg}} = 0$: (1) without ADP, L_N ; (2) max. ATP/ADP ratio, L_T ; or (3) inhibition of the phosphorylation pathway, L_{Omy}
OXPHOS	P ; high ADP-stimulated respiration	max.	high	Kinetically-saturating [ADP] and $[P_i]$	$J_{P_{\gg}}$ by phosphorylation pathway; or $J_{O_2,k}$ by ET-pathway capacity
ET	E ; max. noncoupled respiration	0	low	Optimal external uncoupler concentration for max. oxygen flux	$J_{O_2,k}$ by ET-pathway capacity
ROX	R_{ox} ; min. residual O_2 consumption	0	0	$J_{O_2,R_{ox}}$ in non-ET-pathway oxidation reactions	Full inhibition of ET-pathway or absence of fuel substrates

396

397

398 **LEAK state (Fig. 3):** The
 399 LEAK state is defined as a state
 400 of mitochondrial respiration
 401 when O_2 flux mainly
 402 compensates for the proton leak
 403 in the absence of ATP synthesis,

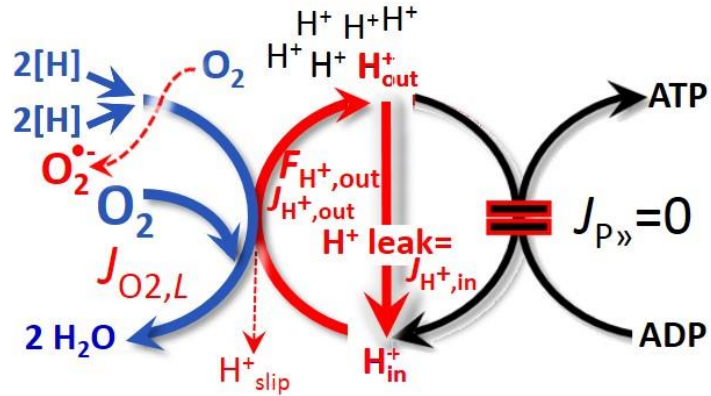


Fig. 3. LEAK state: Phosphorylation is arrested, $J_{P \gg} = 0$, and oxygen flux, $J_{O_2,L}$, is controlled mainly by the proton leak, which equals $J_{H^+,in}$, at maximum protonmotive force, $F_{H^+,out}$ (See also Fig. 2).

404 at kinetically-saturating
 405 concentrations of O_2 and
 406 respiratory substrates. LEAK
 407 respiration is measured to obtain
 408 an indirect estimate of *intrinsic uncoupling* without addition of any experimental uncoupler: (1)
 409 in the absence of adenylates; (2) after depletion of ADP at maximum ATP/ADP ratio; or (3)
 410 after inhibition of the phosphorylation pathway by inhibitors of ATP synthase, such as
 411 oligomycin, or adenine nucleotide translocase, such as carboxyatractyloside.

412

413 **Table 2. Distinction of terms related to coupling.**

Term	Respiration	$P \gg / O_2$	Note
Fully coupled	$P - L$	max.	OXPPOS capacity corrected for LEAK respiration (Fig. 6)
Well coupled	P	high	Phosphorylating respiration with a variable intrinsic LEAK component (Fig. 4)
Loosely coupled	up to E	low	Inducibly uncoupled by UCPI or Ca^{2+} cycling
Dyscoupled	P	low	Pathologically, toxicologically, environmentally increased uncoupling, mitochondrial dysfunction
Uncoupled and decoupled	L	0	Non-phosphorylating intrinsic LEAK respiration without added protonophore (Fig. 3)
Noncoupled	E	0	Non-phosphorylating respiration stimulated to maximum flux at optimum exogenous uncoupler concentration (Fig. 5)

414

415 **Proton leak:** Proton leak is the *uncoupled* process in which protons are translocated
416 across the inner mitochondrial membrane in the dissipative direction of the downhill
417 protonmotive force without coupling to phosphorylation (**Fig. 3**). The proton leak flux depends
418 on the protonmotive force, is a property of the inner mitochondrial membrane, may be enhanced
419 due to possible contaminations by free fatty acids, and is physiologically controlled. In
420 particular, inducible uncoupling mediated by uncoupling protein 1 (UCP1) is physiologically
421 controlled, *e.g.*, in brown adipose tissue. UCP1 is a proton channel of the inner mitochondrial
422 membrane facilitating the conductance of protons across the inner mitochondrial membrane
423 (Klingenberg 2017). As a consequence of this effective short-circuit, the protonmotive force
424 diminishes, resulting in stimulation of electron transfer to oxygen and heat dissipation without
425 phosphorylation of ADP. Mitochondrial injuries may lead to *dyscoupling* as a pathological or
426 toxicological cause of *uncoupled* respiration, *e.g.*, as a consequence of opening the permeability
427 transition pore. Dyscoupled respiration is distinguished from the experimentally induced
428 *noncoupled* respiration in the ET state. Under physiological conditions, the proton leak is the
429 dominant contributor to the overall leak current (Dufour *et al.* 1996).

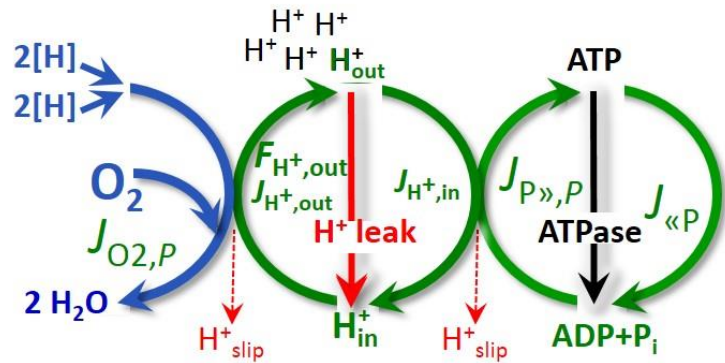
430 **Proton slip:** Proton slip is the *decoupled* process in which protons are only partially
431 translocated by a proton pump of the ET-pathways and slip back to the original compartment
432 (Dufour *et al.* 1996). Proton slip can also happen in association with the ATP-synthase, in which
433 case the proton slips downhill across the membrane to the matrix without contributing to ATP
434 synthesis. In each case, proton slip is a property of the proton pump and increases with the
435 turnover rate of the pump.

436 **Cation cycling:** Proton leak is a leak current of protons. There can be other cation
437 contributors to leak current including calcium and probably magnesium. Calcium current is
438 balanced by mitochondrial Na/Ca exchange, which is balanced by Na/H exchange or K/H
439 exchange. This is another effective uncoupling mechanism different from proton leak and slip.

440 Small differences of terms, *e.g.*, uncoupled, noncoupled, are easily overlooked and may
 441 be erroneously perceived as identical. Even with an attempt at rigorous definition, the common
 442 use of such terms may remain vague (Table 2).

443 **OXPHOS state (Fig. 4):**

444 The OXPHOS state is defined as
 445 the respiratory state with
 446 kinetically-saturating
 447 concentrations of O₂, respiratory
 448 and phosphorylation substrates,
 449 and absence of exogenous
 450 uncoupler, which provides an
 451 estimate of the maximal
 452 respiratory capacity in the



453 **Fig. 4. OXPHOS state:** Phosphorylation, $J_{P\gg,P}$, is stimulated
 454 by kinetically-saturating [ADP] and inorganic phosphate,
 455 [P_i], and is supported by a high protonmotive force, $F_{H^+,out}$.
 456 O₂ flux, $J_{O_2,P}$, is highly coupled at a maximum P_»/O₂ ratio,
 457 $J_{P\gg,P}/J_{O_2,P}$ (See also Fig. 2).

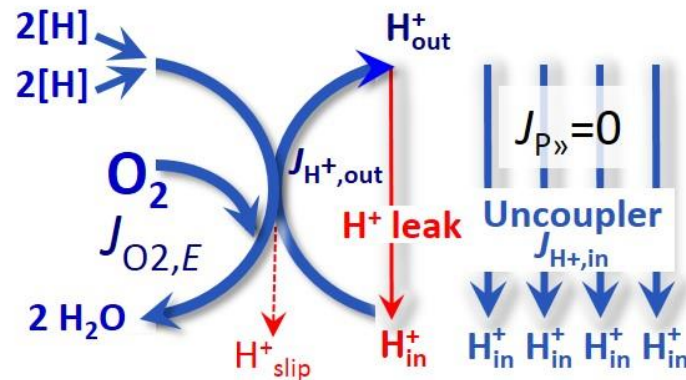
453 OXPHOS state for any given ET-pathway state. Respiratory capacities at kinetically-saturating
 454 substrate concentrations provide reference values or upper limits of performance, aiming at the
 455 generation of data sets for comparative purposes. Any effects of substrate kinetics are thus
 456 separated from reporting actual mitochondrial capacity for oxidation during coupled
 457 respiration, against which physiological activities can be evaluated.

458 As discussed previously, 0.2 mM ADP does not fully saturate flux in isolated
 459 mitochondria (Gnaiger 2001; Puchowicz *et al.* 2004); greater ADP concentration is required,
 460 particularly in permeabilized muscle fibres and cardiomyocytes, to overcome limitations by
 461 intracellular diffusion and by the reduced conductance of the outer mitochondrial membrane
 462 (Jepihhina *et al.* 2011, Illaste *et al.* 2012, Simson *et al.* 2016) either through interaction with
 463 tubulin (Rostovtseva *et al.* 2008) or other intracellular structures (Birkedal *et al.* 2014). In
 464 permeabilized muscle fibre bundles of high respiratory capacity, the apparent K_m for ADP
 465 increases up to 0.5 mM (Saks *et al.* 1998), indicating that >90% saturation is reached only at

466 >5 mM ADP. Similar ADP concentrations are also required for accurate determination of
 467 OXPHOS capacity in human clinical cancer samples and permeabilized cells (Klepinin *et al.*
 468 2016; Koit *et al.* 2017). Whereas 2.5 to 5 mM ADP is sufficient to obtain the actual OXPHOS
 469 capacity in many types of permeabilized cell and tissue preparations, experimental validation
 470 is required in each specific case.

471 Electron transfer state

472 (Fig. 5): The ET state is defined
 473 as the *noncoupled* state with
 474 kinetically-saturating
 475 concentrations of O₂, respiratory
 476 substrate and optimum
 477 exogenous uncoupler
 478 concentration for maximum O₂
 479 flux, as an estimate of oxidative



480 ET capacity. Inhibition of respiration is observed at higher than optimum uncoupler
 481 concentrations. As a consequence of the nearly collapsed protonmotive force, the driving force
 482 is insufficient for phosphorylation and $J_{P_{\gg}} = 0$.
 483 **Fig. 5. ET state:** Noncoupled respiration, $J_{O_2,E}$, is maximum
 484 at optimum exogenous uncoupler concentration and
 485 phosphorylation is zero, $J_{P_{\gg}} = 0$ (See also Fig. 2).

480 ET capacity. Inhibition of respiration is observed at higher than optimum uncoupler
 481 concentrations. As a consequence of the nearly collapsed protonmotive force, the driving force
 482 is insufficient for phosphorylation and $J_{P_{\gg}} = 0$.

483 Besides the three fundamental coupling states of mitochondrial preparations, the
 484 following respiratory state also is relevant to assess respiratory function:

485 **ROX:** Residual oxygen consumption (ROX) is defined as O₂ consumption due to
 486 oxidative side reactions remaining after inhibition of ET with rotenone, malonic acid and
 487 antimycin A. Cyanide and azide not only inhibit CIV but several peroxidases which might be
 488 involved in ROX. ROX is not a coupling state but represents a baseline that is used to correct
 489 mitochondrial respiration in defined coupling states. ROX is not necessarily equivalent to non-
 490 mitochondrial respiration, considering oxygen-consuming reactions in mitochondria not related
 491 to ET, such as oxygen consumption in reactions catalyzed by monoamine oxidases (type A and

492 B), monooxygenases (cytochrome P450 monooxygenases), dioxygenase (sulfur dioxygenase
 493 and trimethyllysine dioxygenase), several hydroxylases, and more. Mitochondrial preparations,
 494 especially those obtained from liver, are contaminated by peroxisomes. This fact makes the
 495 exact determination of mitochondrial oxygen consumption and mitochondria-associated
 496 generation of reactive oxygen species complicated (Schönfeld *et al.* 2009). The dependence of
 497 ROX-linked oxygen consumption needs to be studied in detail with respect to non-ET enzyme
 498 activities, availability of specific substrates, oxygen concentration, and electron leakage leading
 499 to the formation of reactive oxygen species.

500

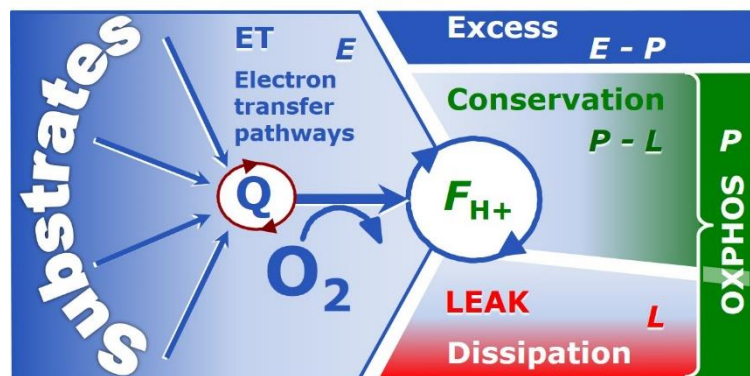
501 2.2. Coupling states and respiratory rates

502 It is important to distinguish metabolic pathways from metabolic states and the
 503 corresponding metabolic rates; for example: electron transfer pathways (Fig. 6), ET state (Fig.
 504 5), and ET capacity, E , respectively (Table 1). The protonmotive force is *high* in the OXPHOS
 505 state when it drives phosphorylation, *maximum* in the LEAK state of coupled mitochondria,
 506 driven by LEAK respiration at a minimum back flux of protons to the matrix side, and *very low*
 507 in the ET state when uncouplers short-circuit the proton cycle (Table 1).

508

509 **Fig. 6. Four-compartment model**
 510 **of oxidative phosphorylation.**

511 Respiratory states (ET, OXPHOS,
 512 LEAK) and corresponding rates (E ,
 513 P , L) are connected by the
 514 protonmotive force, $F_{H+,out}$. Electron
 515 transfer capacity, E , is partitioned



516 into (1) dissipative LEAK respiration, L , when the capacity to perform work is irreversibly lost, (2) net
 517 OXPHOS capacity, $P-L$, with partial conservation of the capacity to perform work, and (3) the excess
 518 capacity, $E-P$. Modified from Gnaiger (2014).

519

520 The three coupling states, ET, LEAK and OXPHOS, are presented in a schematic context
521 with the corresponding respiratory rates, abbreviated as E , L and P , respectively (**Fig. 6**). This
522 clarifies that E may exceed or be equal to P , but E cannot theoretically be lower than P . $E < P$
523 must be discounted as an artefact, which may be caused experimentally by: (1) loss of oxidative
524 capacity during the time course of the respirometric assay, since E is measured subsequently to
525 P ; (2) using insufficient uncoupler concentrations; (3) using high uncoupler concentrations which
526 inhibit ET (Gnaiger 2008); (4) high oligomycin concentrations applied for measurement of L
527 before titrations of uncoupler, when oligomycin exerts an inhibitory effect on E . On the other
528 hand, the excess ET capacity is overestimated if non-saturating $[P_i]$ or $[ADP]$ are used (see State
529 3 in the next section).

530 $E > P$ is observed in many types of mitochondria, varying between species, tissues and
531 cell types. It is the excess ET capacity pushing the phosphorylation pathway flux (**Fig. 1B**) to
532 the limit of its *capacity of utilizing* the protonmotive force. Within any type of mitochondria,
533 the magnitude of $E > P$ depends on (1) the pathway control state with single or multiple electron
534 input into the Q-junction and involvement of three or fewer coupling sites determining the
535 H^+_{out}/O_2 *coupling stoichiometry* (**Fig. 1A**); and (2) the *biochemical coupling efficiency*
536 expressed as $(E-L)/E$, since an increase of L causes P to increase towards the limit of E . The
537 *excess E-P* capacity, $E-P$, therefore, provides a sensitive diagnostic indicator of specific injuries
538 of the phosphorylation pathway, under conditions when E remains constant but P declines
539 relative to controls (**Fig. 6**). Substrate cocktails supporting simultaneous convergent electron
540 transfer to the Q-junction for reconstitution of tricarboxylic acid cycle (TCA cycle) function
541 establish pathway control states with high ET capacity, and consequently increase the
542 sensitivity of the $E-P$ assay.

543 When subtracting L from P , the dissipative LEAK component in the OXPHOS state may
544 be overestimated. This can be avoided by measuring LEAK respiration in a state when the
545 protonmotive force is adjusted to its slightly lower value in the OXPHOS state, *e.g.*, by titration

546 of an ET inhibitor. Any turnover-dependent components of proton leak and slip, however, are
 547 underestimated under these conditions (Garlid *et al.* 1993). In general, it is inappropriate to use
 548 the term *ATP production* or *ATP turnover* for the difference of oxygen consumption measured
 549 in states *P* and *L*. The difference *P-L* is the upper limit of the part of OXPHOS capacity that is
 550 freely available for ATP production (corrected for LEAK respiration) and is fully coupled to
 551 phosphorylation with a maximum mechanistic stoichiometry (**Fig. 6**).

552

553 2.3. Classical terminology for isolated mitochondria

554 *‘When a code is familiar enough, it ceases appearing like a code; one forgets that*
 555 *there is a decoding mechanism. The message is identical with its meaning’*
 556 (Hofstadter 1979).

557 Chance and Williams (1955; 1956) introduced five classical states of mitochondrial respiration
 558 and cytochrome redox states. **Table 3** shows a protocol with isolated mitochondria in a closed
 559 respirometric chamber, defining a sequence of respiratory states.

560 **Table 3. Metabolic states of mitochondria (Chance and**
 561 **Williams, 1956; Table V).**
 562

State	[O ₂]	ADP level	Substrate level	Respiration rate	Rate-limiting substance
1	>0	low	low	slow	ADP
2	>0	high	~0	slow	substrate
3	>0	high	high	fast	respiratory chain
4	>0	low	high	slow	ADP
5	0	high	high	0	oxygen

563

564 **State 1** is obtained after addition of isolated mitochondria to air-saturated
 565 isoosmotic/isotonic respiration medium containing inorganic phosphate, but no fuel substrates
 566 and no adenylates, *i.e.*, AMP, ADP, ATP.

567 **State 2** is induced by addition of a high concentration of ADP (typically 100 to 300 μ M),
 568 which stimulates respiration transiently on the basis of endogenous fuel substrates and

569 phosphorylates only a small portion of the added ADP. State 2 is then obtained at a low
570 respiratory activity limited by zero endogenous fuel substrate availability (**Table 3**). If addition
571 of specific inhibitors of respiratory complexes, such as rotenone, does not cause a further
572 decline of oxygen consumption, State 2 is equivalent to residual oxygen consumption (See
573 below). If inhibition is observed, undefined endogenous fuel substrates are a confounding factor
574 of pathway control by externally added substrates and inhibitors. In contrast to the original
575 protocol, an alternative sequence of titration steps is frequently applied, in which the alternative
576 State 2 has an entirely different meaning, when this second state is induced by addition of fuel
577 substrate without ADP (LEAK state; in contrast to State 2 defined in **Table 2** as a ROX state),
578 followed by addition of ADP.

579 **State 3** is the state stimulated by addition of fuel substrates while the ADP concentration
580 is still high (**Table 3**) and supports coupled energy transformation through oxidative
581 phosphorylation. 'High ADP' is a concentration of ADP specifically selected to allow the
582 measurement of State 3 to State 4 transitions of isolated mitochondria in a closed respirometric
583 chamber. Repeated ADP titration re-establishes State 3 at 'high ADP'. Starting at oxygen
584 concentrations near air-saturation (ca. 200 μM O_2 at sea level and 37 $^\circ\text{C}$), the total ADP
585 concentration added must be low enough (typically 100 to 300 μM) to allow phosphorylation
586 to ATP at a coupled oxygen consumption that does not lead to oxygen depletion during the
587 transition to State 4. In contrast, kinetically-saturating ADP concentrations usually are an order
588 of magnitude higher than 'high ADP', *e.g.* 2.5 mM in isolated mitochondria. The abbreviation
589 State 3u is frequently used in bioenergetics, to indicate the state of respiration after titration of
590 an uncoupler, without sufficient emphasis on the fundamental difference between OXPHOS
591 capacity (*well-coupled* with an *endogenous* uncoupled component) and ET capacity
592 (*noncoupled*).

593 **State 4** is a LEAK state that is obtained only if the mitochondrial preparation is intact and
594 well-coupled. Depletion of ADP by phosphorylation to ATP leads to a decline in oxygen

595 consumption in the transition from State 3 to State 4. Under these conditions, a maximum
 596 protonmotive force and high ATP/ADP ratio are maintained, and the P_{O_2} ratio can be
 597 calculated. State 4 respiration, L_T (**Table 1**), reflects intrinsic proton leak and intrinsic ATP
 598 hydrolysis activity. Oxygen consumption in State 4 is an overestimation of LEAK respiration
 599 if the contaminating ATP hydrolysis activity recycles some ATP to ADP, J_{ATP} , which stimulates
 600 respiration coupled to phosphorylation, $J_{\text{P}} > 0$. This can be tested by inhibition of the
 601 phosphorylation pathway using oligomycin, ensuring that $J_{\text{P}} = 0$ (State 4o). Alternatively,
 602 sequential ADP titrations re-establish State 3, followed by State 3 to State 4 transitions while
 603 sufficient oxygen is available. However, anoxia may be reached before exhaustion of ADP
 604 (State 5).

605 **State 5** is the state after exhaustion of oxygen in a closed respirometric chamber.
 606 Diffusion of oxygen from the surroundings into the aqueous solution may be a confounding
 607 factor preventing complete anoxia (Gnaiger 2001). Chance and Williams (1955) provide an
 608 alternative definition of State 5, which gives it the meaning of ROX: ‘State 5 may be obtained
 609 by antimycin A treatment or by anaerobiosis’.

610 In **Table 3**, only States 3 and 4 (and ‘State 2’ in the alternative protocol without ADP;
 611 not included in the table) are coupling control states, with the restriction that O_2 flux in State 3
 612 may be limited kinetically by non-saturating ADP concentrations (**Table 1**).

613

614 **3. The protonmotive force and proton flux**

615 *3.1. Electric and chemical partial forces versus electrical and chemical units*

616 The protonmotive force across the inner mitochondrial membrane (Mitchell and Moyle
 617 1967) was introduced most beautifully in the *Grey Book 1966* (see Mitchell 2011),

$$618 \quad \Delta p_{\text{H}^+} = \Delta \Psi + \Delta \mu_{\text{H}^+}/F \quad (\text{Eq. 1})$$

619 The protonmotive force consists of two partial forces: (1) The electrical part, $\Delta \Psi$, is the
 620 difference of charge (electric potential difference) and is not specific for H^+ . (2) The chemical

621 part, $\Delta\mu_{H^+}$, is the chemical potential difference in H^+ , is proportional to the pH difference, and
 622 incorporates the Faraday constant (**Table 4**).

623
 624 **Table 4. Protonmotive force and flux matrix.** Rows: Electrical and chemical
 625 isomorphic format (e and n). The Faraday constant, F , converts protonmotive force
 626 and flux from *isomorphic format* e to n . Columns: The protonmotive force is the sum of
 627 *partial isomorphic forces* F_{el} and $F_{H^+,d}$. In contrast to force (state), the conjugated flux
 628 (rate) cannot be partitioned.
 629

State	Force	electric	+	chem.	Unit	Notes	
Protonmotive force, e	Δp_{H^+}	=	$\Delta\Psi$	+ $\Delta\mu_{H^+}/F$	$J\cdot C^{-1}$	$1e$	
Chemiosmotic potential, n	$\Delta\tilde{\mu}_{H^+}$	=	$\Delta\Psi\cdot F$	+ $\Delta\mu_{H^+}$	$J\cdot mol^{-1}$	$1n$	
State	Isomorphic force		$F_{H^+,out/i}$	el _{out}	+	H^+ _{out,d}	
Electric charge, e	$F_{H^+,out/e}$	=	$F_{el,out/e}$	+	$F_{H^+,out,d/e}$	$J\cdot C^{-1}$	$2e$
Amount of substance, n	$F_{H^+,out/n}$	=	$F_{el,out/n}$	+	$F_{H^+,out,d/n}$	$J\cdot mol^{-1}$	$2n$
Rate	Isomorphic flux		$J_{H^+,out/i}$	e	or	n	
Electric charge, e	$J_{H^+,out/e}$		$J_{H^+,out/e}$			$C\cdot s^{-1}\cdot m^{-3}$	$3e$
Amount of substance, n	$J_{H^+,out/n}$				$J_{H^+,out/n}$	$mol\cdot s^{-1}\cdot m^{-3}$	$3n$

630
 631 1: The Faraday constant, F , is the product of elementary charge ($e = 1.602177\cdot 10^{-19}\cdot C$) and the
 632 Avogadro (Loschmidt) constant ($N_A = 6.022136\cdot 10^{23}\cdot mol^{-1}$), $F = eN_A = 96,485.3 C/mol$. $\Delta\tilde{\mu}_{H^+}$ is the
 633 chemiosmotic potential difference. $1e$ and $1n$ are the classical representations of $2e$ and $2n$.
 634 2: The protonmotive force is $F_{H^+,out}$, expressed either in isomorphic format e or n . $F_{el/e}\equiv\Delta\Psi$ is the partial
 635 protonmotive force (el) acting generally on charged motive molecules (*i.e.* ions that are displaceable
 636 across the inner mitochondrial membrane). In contrast, $F_{H^+,d/n}\equiv\Delta\mu_{H^+}$ is the partial protonmotive force
 637 specific for proton displacement (H^+_d). The sign of the force is negative for exergonic transformations
 638 in which exergy is lost or dissipated, and positive for endergonic transformations which conserve
 639 exergy from a coupled exergonic process (**Box 3**).
 640 3: The sign of the flux depends on the definition of the compartmental direction of the translocation (**Fig.**
 641 **2**). Flux x force = $J_{H^+,out/e}\cdot F_{H^+,out/e} = J_{H^+,out/n}\cdot F_{H^+,out/n} =$ volume-specific power [$J\cdot s^{-1}\cdot m^{-3} = W\cdot m^{-3}$].
 642

643 **Faraday constant**, $F = eN_A$ [C/mol] (**Table 4**), enables the conversion between
 644 protonmotive force, $F_{H^+,out/e} \equiv \Delta p_{H^+}$ [J/C], expressed per *motive charge*, e [C], and protonmotive
 645 force or electrochemical potential difference, $F_{H^+,out/n} \equiv \Delta \tilde{\mu}_{H^+} = \Delta p_{H^+} \cdot F$ [J/mol], expressed per
 646 *motive amount of protons*, n [mol]. Proton charge, e , and amount of substance, n , define the
 647 units for the isomorphic formats. Taken together, F converts protonmotive force and flux from
 648 isomorphic format e to n (Eq. 2; see also **Table 4**, Note 2),

$$649 \quad F_{H^+,out/n} = F_{H^+,out/e} \cdot eN_A \quad (\text{Eq. 2.1})$$

$$650 \quad J_{H^+,out/n} = J_{H^+,out/e} / (eN_A) \quad (\text{Eq. 2.2})$$

651 In each format, the protonmotive force is expressed as the sum of two partial forces. The
 652 concept expressed by the complex symbols in Eq. 1 can be explained and visualized more easily
 653 by *partial isomorphic forces* as the components of the protonmotive force:

654 **Electrical part of the protonmotive force:** (1) Isomorph e : $F_{el/e} \equiv \Delta \Psi$ is the electrical
 655 part of the protonmotive force expressed in units joule per coulomb, *i.e.* volt [$V = J/C$]. $F_{el/e}$ is
 656 defined as partial Gibbs energy change per *motive elementary charge*, e [C], not specific for
 657 proton charge (**Table 4**, Note 2e). (2) Isomorph n : $F_{el/n} \equiv \Delta \Psi \cdot F$ is the electric force expressed
 658 in units joule per mole [J/mol], defined as partial Gibbs energy change per *motive amount of*
 659 *charge*, n [mol], not specific for proton charge (**Table 4**, Note 2n).

660 **Chemical part of the protonmotive force:** (1) Isomorph n : $F_{d,H^+/n} \equiv \Delta \mu_{H^+}$ is the chemical
 661 part (diffusion, displacement of H^+) of the protonmotive force expressed in units joule per mole
 662 [J/mol]. $F_{d,H^+/n}$ is defined as partial Gibbs energy change per *motive amount of protons*, n [mol]
 663 (**Table 4**, Note 2n). (2) Isomorph e : $F_{d,H^+/e} \equiv \Delta \mu_{H^+} / F$ is the chemical force expressed in units
 664 joule per coulomb [V], defined as partial Gibbs energy change per *motive amount of protons*
 665 *expressed in units of electric charge*, e [C], but specific for proton charge (**Table 4**, Note 2e).

666 Protonmotive means that there is a potential for the movement of protons, and force is a
 667 measure of the potential for motion. Motion is relative and not absolute (Principle of Galilean
 668 Relativity); likewise there is no absolute potential, but (isomorphic) forces are potential

669 differences. An electric partial force expressed in the format of electric charge, $F_{el/e}$, of -0.2 V
670 (**Table 5**, Note 5e) is equivalent to force in the format of amount, $F_{el,H+/n}$, of $19 \text{ kJ}\cdot\text{mol}^{-1} \text{ H}^+_{\text{out}}$
671 (Note 5n). For a ΔpH of 1 unit, the chemical partial force in the format of amount, $F_{d,H+/n}$,
672 changes by $5.9 \text{ kJ}\cdot\text{mol}^{-1}$ (**Table 5**, Note 6n) and chemical force in the format of charge $F_{d,H+/e}$
673 changes by 0.06 V (Note 6e). Considering a driving force of $-470 \text{ kJ}\cdot\text{mol}^{-1} \text{ O}_2$ for oxidation, the
674 thermodynamic limit of the $\text{H}^+_{\text{out}}/\text{O}_2$ ratio is reached at a value of $470/19 = 24$, compared to a
675 mechanistic stoichiometry of 20 (**Fig. 1**).

676

677 3.2. Definitions

678 **Control and regulation:** The terms metabolic *control* and *regulation* are frequently used
679 synonymously, but are distinguished in metabolic control analysis: ‘We could understand the
680 regulation as the mechanism that occurs when a system maintains some variable constant over
681 time, in spite of fluctuations in external conditions (homeostasis of the internal state). On the
682 other hand, metabolic control is the power to change the state of the metabolism in response to
683 an external signal’ (Fell 1997). Respiratory control may be induced by experimental control
684 signals that *exert* an influence on: (1) ATP demand and ADP phosphorylation rate; (2) fuel
685 substrate composition, pathway competition; (3) available amounts of substrates and oxygen,
686 *e.g.*, starvation and hypoxia; (3) the protonmotive force, redox states, flux-force relationships,
687 coupling and efficiency; (4) Ca^{2+} and other ions including H^+ ; (5) inhibitors, *e.g.*, nitric oxide
688 or intermediary metabolites, such as oxaloacetate; (6) signalling pathways and regulatory
689 proteins, *e.g.* insulin resistance, transcription factor HIF-1 or inhibitory factor 1. *Mechanisms*
690 of respiratory control and regulation include adjustments of (1) enzyme activities by allosteric
691 mechanisms and phosphorylation, (2) enzyme content, concentrations of cofactors and
692 conserved moieties (such as adenylates, nicotinamide adenine dinucleotide [NAD^+/NADH],
693 coenzyme Q, cytochrome *c*); (3) metabolic channeling by supercomplexes; and (4)
694 mitochondrial density (enzyme concentrations and membrane area) and morphology (cristae

695 folding, fission and fusion). (5) Mitochondria are targeted directly by hormones, thereby
696 affecting their energy metabolism (Lee *et al.* 2013; Gerö and Szabo 2016; Price and Dai 2016;
697 Moreno *et al.* 2017). Evolutionary or acquired differences in the genetic and epigenetic basis
698 of mitochondrial function (or dysfunction) between subjects and gene therapy; age; gender,
699 biological sex, and hormone concentrations; life style including exercise and nutrition; and
700 environmental issues including thermal, atmospheric, toxicological and pharmacological
701 factors, exert an influence on all control mechanisms listed above (for reviews, see Brown 1992;
702 Gnaiger 1993a, 2009; 2014; Paradies *et al.* 2014; Morrow *et al.* 2017).

703 **Respiratory control and response:** Lack of control by a metabolic pathway, *e.g.*
704 phosphorylation pathway, does mean that there will be no response to a variable activating it,
705 *e.g.* [ADP]. However, the reverse is not true as the absence of a response to [ADP] does not
706 exclude the phosphorylation pathway from having some degree of control. The degree of
707 control of a component of the OXPHOS pathway on an output variable, such as oxygen flux,
708 will in general be different from the degree of control on other outputs, such as phosphorylation
709 flux or proton leak flux (**Box 2**). As such, it is necessary to be specific as to which input and
710 output are under consideration (Fell 1997). Therefore, the term respiratory control is elaborated
711 in more detail in the following section.

712 **Respiratory coupling control:** Respiratory control refers to the ability of mitochondria
713 to adjust oxygen consumption in response to external control signals by engaging various
714 mechanisms of control and regulation. Respiratory control is monitored in a mitochondrial
715 preparation under conditions defined as respiratory states. When phosphorylation of ADP to
716 ATP is stimulated or depressed, an increase or decrease is observed in electron flux linked to
717 oxygen consumption in respiratory coupling states of intact mitochondria ('controlled states' in
718 the classical terminology of bioenergetics). Alternatively, coupling of electron transfer with
719 phosphorylation is disengaged by disruption of the integrity of the inner mitochondrial
720 membrane or by uncouplers, functioning like a clutch in a mechanical system. The

721 corresponding coupling control state is characterized by high levels of oxygen consumption
 722 without control by phosphorylation ('uncontrolled state'). Energetic coupling is defined in **Box**
 723 **4**. Loss of coupling lowers the efficiency by intrinsic uncoupling and decoupling, or
 724 pathological dyscoupling. Such generalized uncoupling is different from switching to
 725 mitochondrial pathways that involve fewer than three proton pumps ('coupling sites':
 726 Complexes CI, CIII and CIV), bypassing CI through multiple electron entries into the Q-
 727 junction (**Fig. 1**). A bypass of CIII and CIV is provided by alternative oxidases, which reduce
 728 oxygen without proton translocation. Reprogramming of mitochondrial pathways may be
 729 considered as a switch of gears (changing the stoichiometry) rather than uncoupling (loosening
 730 the stoichiometry).

731 **Pathway control states** are obtained in mitochondrial preparations by depletion of
 732 endogenous substrates and addition to the mitochondrial respiration medium of fuel substrates
 733 (CHNO) and specific inhibitors, activating selected mitochondrial pathways (**Fig. 1**). Coupling
 734 control states and pathway control states are complementary, since mitochondrial preparations
 735 depend on an exogenous supply of pathway-specific fuel substrates and oxygen (Gnaiger 2014).

736

737 **Box 2: Metabolic fluxes and flows: vectorial and scalar**

738 In mitochondrial electron transfer (**Fig. 1**), vectorial transmembrane proton flux is coupled
 739 through the proton pumps CI, CIII and CIV to the catabolic flux of scalar reactions, collectively
 740 measured as oxygen flux. In **Fig. 2**, the scalar catabolic reaction, k , of oxygen consumption,
 741 $J_{O_2,k}$ [$\text{mol}\cdot\text{s}^{-1}\cdot\text{m}^{-3}$], is expressed as oxygen flux per volume, V [m^3], of the instrumental chamber
 742 (the system).

743 Fluxes are *vectors*, if they have *spatial* direction in addition to magnitude. A vector flux
 744 (surface-density of flow) is expressed per unit cross-sectional area, A [m^2], perpendicular to the
 745 direction of flux. If *flows*, I , are defined as extensive quantities of the *system*, as vector or scalar
 746 flow, I or I [$\text{mol}\cdot\text{s}^{-1}$], respectively, then the corresponding vector and scalar *fluxes*, J , are

747 obtained as $J = I \cdot A^{-1}$ [$\text{mol} \cdot \text{s}^{-1} \cdot \text{m}^{-2}$] and $J = I \cdot V^{-1}$ [$\text{mol} \cdot \text{s}^{-1} \cdot \text{m}^{-3}$], respectively, expressing flux as an
 748 area-specific vector or volume-specific scalar quantity.

749 Vectorial transmembrane proton flux, $J_{\text{H}^+, \text{out}}$, is analyzed in a heterogenous
 750 compartmental system as a quantity with *directional* but not *spatial* information. Translocation
 751 of protons across the inner mitochondrial membrane has a defined direction, either from the
 752 negative compartment (matrix space; negative or $\bar{\text{C}}$ Compartment) to the positive compartment
 753 (inter-membrane space; positive or C Compartment) or *vice versa* (**Fig. 2**). The arrows defining
 754 the direction of the translocation between the two compartments may point upwards or
 755 downwards, right or left, without any implication that these are actual directions in space. The
 756 ‘upper’ compartment of the C Compartment is neither above nor below the $\bar{\text{C}}$ Compartment in a
 757 spatial sense, but can be visualized arbitrarily in a figure as the upper compartment (**Fig. 2**). In
 758 general, the *compartmental direction* of vectorial translocation from the $\bar{\text{C}}$ Compartment to the
 759 C Compartment is defined by assigning the initial and final state as *ergodynamic compartments*,
 760 $\text{H}^+_{\text{in}} \rightarrow \text{H}^+_{\text{out}}$, respectively, related to work (erg = work) that must be performed to lift the proton
 761 from a lower to a higher electrochemical potential or from the lower to the higher ergodynamic
 762 compartment (Gnaiger 1993b).

763 In direct analogy to *vectorial* translocation, the direction of a *scalar* chemical reaction, A
 764 $\rightarrow \text{B}$, is defined by assigning substrates and products, A and B, as ergodynamic compartments.
 765 O_2 is defined as a substrate in respiratory O_2 consumption, which together with the fuel
 766 substrates comprises the substrate compartment of the catabolic reaction (**Fig. 2**). Volume-
 767 specific scalar O_2 flux is coupled (**Box 4**) to vectorial translocation. In order to establish a
 768 quantitative relation between the coupled fluxes, both $J_{\text{O}_2, \text{k}}$ and $J_{\text{H}^+, \text{out}}$ must be expressed in
 769 identical units ($[\text{mol} \cdot \text{s}^{-1} \cdot \text{m}^{-3}]$ or $[\text{C} \cdot \text{s}^{-1} \cdot \text{m}^{-3}]$), yielding the $\text{H}^+_{\text{out}}/\text{O}_2$ ratio (**Fig. 1**). The *vectorial*
 770 proton flux in compartmental translocation has *compartmental direction*, distinguished from a
 771 *vector* flux with *spatial direction*. Likewise, the corresponding protonmotive force is defined

772 as an electrochemical potential *difference* between two compartments, in contrast to a *gradient*
 773 across the membrane or a vector force with defined spatial direction.

774

775 **The steady-state:** Mitochondria represent a thermodynamically open system functioning
 776 as a biochemical transformation system in non-equilibrium states. State variables (protonmotive
 777 force; redox states) and metabolic fluxes (*rates*) are measured in defined mitochondrial
 778 respiratory *states*. Strictly, steady states can be obtained only in open systems, in which changes
 779 due to *internal* transformations, *e.g.*, O₂ consumption, are instantaneously compensated for by
 780 *external* fluxes *e.g.*, O₂ supply, such that oxygen concentration does not change in the system
 781 (Gnaiger 1993b). Mitochondrial respiratory states monitored in closed systems satisfy the
 782 criteria of pseudo-steady states for limited periods of time, when changes in the system
 783 (concentrations of O₂, fuel substrates, ADP, P_i, H⁺) do not exert significant effects on metabolic
 784 fluxes (respiration, phosphorylation). Such pseudo-steady states require respiratory media with
 785 sufficient buffering capacity and kinetically-saturating concentrations of substrates to be
 786 maintained, and thus depend on the kinetics of the processes under investigation. Proton
 787 turnover, $J_{\infty H^+}$, and ATP turnover, $J_{\infty P}$, proceed in the steady-state at constant $F_{H^+,out}$, when $J_{\infty H^+}$
 788 $= J_{H^+,out} = J_{H^+,in}$, and at constant $F_{P\gg}$, when $J_{\infty P} = J_{P\gg} = J_{\ll P}$ (**Fig. 2**).

789

790 **Box 3: Endergonic and exergonic transformations, exergy and dissipation**

791 A chemical reaction, or any transformation, is exergonic if the Gibbs energy change (exergy)
 792 of the reaction is negative at constant temperature and pressure. The sum of Gibbs energy
 793 changes of all internal transformations in a system can only be negative, *i.e.* exergy is
 794 irreversibly dissipated. Endergonic reactions are characterized by positive Gibbs energies of
 795 reaction and cannot proceed spontaneously in the forward direction as defined. For instance,
 796 the endergonic reaction P \gg is coupled to exergonic catabolic reactions, such that the total Gibbs
 797 energy change is negative, *i.e.* exergy must be dissipated for the reaction to proceed (**Fig. 2**).

798 In contrast, energy cannot be lost or produced in any internal process, which is the key
 799 message of the first law of thermodynamics. Thus mitochondria are the sites of energy
 800 transformation but not energy production. Open and closed systems can gain energy and exergy
 801 only by external fluxes, *i.e.* uptake from the environment. Exergy is the potential to perform
 802 work. In the framework of flux-force relationships (**Box 4**), the *partial* derivative of Gibbs
 803 energy per advancement of a transformation is an isomorphic force, F_{tr} (**Table 5**, Note 2). In
 804 other words, force is equal to exergy/motive unit (in integral form, this definition takes care of
 805 non-isothermal processes). This formal generalization represents an appreciation of the
 806 conceptual beauty of Peter Mitchell's innovation of the protonmotive force against the
 807 background of the established paradigm of the electromotive force (emf) defined at the limit of
 808 zero current (Cohen *et al.* 2008).

809

810

811 **Table 5. Power, exergy, force, flux, and advancement.**

812

Expression	Symbol	Definition	Unit	Notes
Power, volume-specific	$P_{V,tr}$	$P_{V,tr} = J_{tr} \cdot F_{tr} = \hat{\partial}_{tr}G \cdot \partial t^{-1}$	$W = J \cdot s^{-1} \cdot m^{-3}$	1
Force, isomorphic	F_{tr}	$F_{tr} = \hat{\partial}_{tr}G \cdot \partial_{tr}\xi^{-1}$	$J \cdot x^{-1}$	2
Flux, isomorphic	J_{tr}	$J_{tr} = d_{tr}\xi \cdot dt^{-1} \cdot V^{-1}$	$x \cdot s^{-1} \cdot m^{-3}$	3
Advancement, n	$d_{tr}\xi_{H+/n}$	$d_{tr}\xi_{H+/n} = d_{tr}n_{H+} \cdot v_{H+}^{-1}$	mol	$4n$
Advancement, e	$d_{tr}\xi_{H+/e}$	$d_{tr}\xi_{H+/e} = d_{tr}e_{H+} \cdot v_{H+}^{-1}$	C	$4e$
Electric partial force, e	$F_{el/e}$	$F_{el/e} \equiv \Delta\Psi$	V	$5e$
Electric partial force, n	$F_{el/n}$	$\Delta\Psi \cdot F = 96.5 \cdot \Delta\Psi$	$kJ \cdot mol^{-1}$	$5n$
Chemical partial force, e	$F_{d,H+/e}$	$\Delta\mu_{H+}/F =$ $-\ln(10) \cdot RT/F \cdot \Delta pH$	V	$6e$
		at 37 °C $= -0.06 \cdot \Delta pH$	$J \cdot C^{-1}$	
Chemical partial force, n	$F_{d,H+/n}$	$\Delta\mu_{H+} = -\ln(10) \cdot RT \cdot \Delta pH$	$J \cdot mol^{-1}$	$6n$
		at 37 °C $= -5.9 \cdot \Delta pH$	$kJ \cdot mol^{-1}$	

813

814 1 to 4: An isomorphic motive entity or transformant, expressed in units x , is defined for any815 transformation, tr. $x = \text{mol}$ or C in proton translocation.

- 816 2: $\partial_{tr}G$ [J] is the partial Gibbs energy change in the advancement of transformation tr.
- 817 3: For $x = C$, flow is electric current, I_{el} [A = C·s⁻¹], vector flux is electric current density per area, \mathbf{J}_{el} ,
- 818 and compartmental flux is electric current density per volume, I_{el} [A·m⁻³].
- 819 4n: For a chemical reaction, the advancement of reaction r is $d_r\xi_B = d_r n_B \cdot v_B^{-1}$ [mol]. The stoichiometric
- 820 number is $v_B = -1$ or $v_B = 1$, depending on B being a product or substrate, respectively, in reaction
- 821 r involving one mole of B. The conjugated *intensive* molar quantity, $F_{B,r} = \partial_r G / \partial_r \xi_B$ [J·mol⁻¹], is the
- 822 chemical force of reaction or *reaction-motive* force per stoichiometric amount of B. In reaction
- 823 kinetics, $d_r n_B$ is expressed as a volume-specific quantity, which is the partial contribution to the
- 824 total concentration change of B, $d_r c_B = d_r n_B / V$ and $dc_B = dn_B / V$, respectively. In open systems with
- 825 constant volume V , $dc_B = d_r c_B + d_e c_B$, where r indicates the *internal* reaction and e indicates the
- 826 *external* flux of B into the unit volume of the system. At steady state the concentration does not
- 827 change, $dc_B = 0$, when $d_r c_B$ is compensated for by the external flux of B, $d_r c_B = -d_e c_B$ (Gnaiger
- 828 1993b). Alternatively, $dc_B = 0$ when B is held constant by different coupled reactions in which B
- 829 acts as a substrate or a product.
- 830 4e: Scalar potential difference across the mitochondrial membrane. In a scalar electric transformation
- 831 (flux of charge, *i.e.* volume-specific current, from the matrix space to the intermembrane and
- 832 extramitochondrial space) the motive force is the difference of charge (**Box 2**). The endergonic
- 833 direction of translocation is defined in **Fig. 2** as $H^{+}_{in} \rightarrow H^{+}_{out}$.
- 834 5n: $F = 96.5$ (kJ·mol⁻¹)/V.
- 835 6: The electric partial force is independent of temperature (Note 5), but the chemical partial force
- 836 depends on absolute temperature, T [K].
- 837 6e: RT is the gas constant times absolute temperature. $\ln(10) \cdot RT / F = 59.16$ and 61.54 mV at 298.15
- 838 and 310.15 K (25 and 37 °C), respectively.
- 839 6n: $\ln(10) \cdot RT = 5.708$ and 5.938 kJ·mol⁻¹ at 298.15 and 310.15 K (25 and 37 °C), respectively.

840

841 3.3. Forces and fluxes in physics and irreversible thermodynamics

842 According to its definition in physics, a potential difference and as such the

843 *protonmotive force*, Δp_{H^+} , is not a force *per se* (Cohen *et al.* 2008). The fundamental forces of

844 physics are distinguished from *motive forces* of statistical and irreversible thermodynamics.

845 Complementary to the attempt towards unification of fundamental forces defined in physics,

846 the concepts of Nobel laureates Lars Onsager, Erwin Schrödinger, Ilya Prigogine and Peter
847 Mitchell (even if expressed in apparently unrelated terms) unite the diversity of *generalized* or
848 ‘isomorphic’ *flux-force* relationships, the product of which links to the dissipation function and
849 Second Law of thermodynamics (Schrödinger 1944; Prigogine 1967). A *motive force* is the
850 derivative of potentially available or ‘free’ energy (exergy) per isomorphic *motive* unit (**Box 3**).
851 Perhaps the first account of a *motive force* in energy transformation can be traced back to the
852 Peripatetic school around 300 BC in the context of moving a lever, up to Newton’s motive force
853 proportional to the alteration of motion (Coopersmith 2010).

854 **Vectorial and scalar forces, and fluxes:** In chemical reactions and osmotic or diffusion
855 processes occurring in a closed heterogeneous system, such as a chamber containing isolated
856 mitochondria, scalar transformations occur without measured spatial direction but between
857 separate compartments (translocation between the matrix and intermembrane space) or between
858 energetically-separated chemical substances (reactions from substrates to products). Hence, the
859 corresponding fluxes are not vectorial but scalar, and are expressed per volume and not per
860 membrane area (**Box 2**). The corresponding motive forces are also scalar potential *differences*
861 across the membrane (**Table 5**), without taking into account the *gradients* across the 6 nm thick
862 inner mitochondrial membrane (Rich 2003).

863 **Coupling:** In energetics (ergodynamics), coupling is defined as an energy transformation
864 fuelled by an exergonic (downhill) input process driving the advancement of an endergonic
865 (uphill) output process. The (negative) output/input power ratio is the efficiency of a coupled
866 energy transformation (**Box 4**). At the limit of maximum efficiency of a completely coupled
867 system, the (negative) input power equals the (positive) output power, such that the total power
868 approaches zero at the maximum efficiency of 1, and the process becomes fully reversible
869 without any dissipation of exergy, *i.e.* without entropy production.

870

871

872

873 **Box 4: Coupling, power and efficiency, at constant temperature and pressure**

874 Energetic coupling means that two processes of energy transformation are linked such that the
 875 input power, P_{in} , is the driving element of the output power, P_{out} , and the out/input power ratio
 876 is the efficiency. In general, power is work per unit time [$J \cdot s^{-1} = W$]. When describing a system
 877 with volume V without information on the internal structure, the output is defined as the *external*
 878 work (exergy) performed by the *total* system on its environment. Such a system may be open
 879 for any type of exchange, or closed and thus allowing only heat and work to be exchanged
 880 across the system boundaries. This is the classical black box approach of thermodynamics. In
 881 contrast, in a colourful compartmental analysis of *internal* energy transformations (**Fig. 2**), the
 882 system is structured and described by definition of ergodynamic compartments (with
 883 information on the heterogeneity of the system; **Box 2**) and analysis of separate parts, *i.e.* a
 884 sequence of *partial* energy transformations, tr . In general, power per unit volume, P_{tr}/V [$W \cdot L^{-1}$],
 885 is the product of a volume-specific flux, J_{tr} , and its conjugated force, F_{tr} , and is closely linked
 886 to the dissipation function using the terminology of irreversible thermodynamics (Prigogine
 887 1967; Gnaiger 1993a,b). Output power of proton translocation and catabolic input power are
 888 (**Fig. 2**),

889 Output:
$$P_{H^+,out}/V = J_{H^+,out} \cdot F_{H^+,out}$$

890 Input:
$$P_k/V = J_{O_2,k} \cdot F_{O_2,k}$$

891 $F_{O_2,k}$ is the exergonic input force with a negative sign, and, $F_{H^+,out}$, is the endergonic output
 892 force with a positive sign (**Box 3**). Ergodynamic efficiency is the ratio of output/input power,
 893 or the flux ratio times force ratio (Gnaiger 1993a,b),

894
$$\varepsilon = \frac{P_{H^+,out}}{-P_k} = \frac{J_{H^+,out}}{J_{O_2,k}} \cdot \frac{F_{H^+,out}}{-F_{O_2,k}}$$

895 The concept of incomplete coupling relates exclusively to the first term, *i.e.* the flux ratio, or
 896 H^+_{out}/O_2 ratio (**Fig. 1**). Likewise, respirometric definitions of the P_{\gg}/O_2 ratio and biochemical

897 coupling efficiency (Section 3.2) consider flux ratios. In a completely coupled process, the
898 power efficiency, ε , depends entirely on the force ratio, ranging from zero efficiency at an
899 output force of zero, to the limiting output force and maximum efficiency of 1.0, when the total
900 power of the coupled process, $P_t = P_k + P_{H^+,out}$, equals zero, and any net flows are zero at
901 ergodynamic equilibrium of a coupled process. Thermodynamic equilibrium is defined as the
902 state when all potentials (all forces) are dissipated and equilibrate towards their minima of zero.
903 In a fully or completely coupled process, output and input fluxes are directly proportional in a
904 fixed ratio technically defined as a stoichiometric relationship (a gear ratio in a mechanical
905 system). Such maximal stoichiometric output/input flux ratios are considered in OXPHOS
906 analysis as the upper limits or mechanistic H^+_{out}/O_2 and P_{\gg}/O_2 ratios (**Fig. 1**).

907

908 **Coupled versus bound processes:** Since the chemiosmotic theory describes the
909 mechanisms of coupling in OXPHOS, it may be interesting to ask if the electrical and chemical
910 parts of proton translocation are coupled processes. This is not the case according to the
911 definition of coupling. If the coupling mechanism is disengaged, the output process becomes
912 independent of the input process, and both proceed in their downhill (exergonic) direction (**Fig.**
913 **2**). It is not possible to physically uncouple the electrical and chemical processes, which are
914 only *theoretically* partitioned as electrical and chemical components and can be measured
915 separately. If partial processes are non-separable, *i.e.*, cannot be uncoupled, then these are not
916 *coupled* but are defined as *bound* processes. The electrical and chemical parts are tightly bound
917 partial forces of the protonmotive force, since a flux cannot be partitioned but expressed only
918 in either an electrical or chemical isomorphic format (**Table 4**).

919

920 **4. Normalization: fluxes and flows**

921 The challenges of measuring mitochondrial respiratory flux are matched by those of
922 normalization, whereby O_2 consumption may be considered as the numerator and normalization

923 as the complementary denominator, which are tightly linked in reporting the measurements in
924 a format commensurate with the requirements of a database.

925

926 4.1. Flux per chamber volume

927 When the reactor volume does not change during the reaction, which is typical for liquid
928 phase reactions, the volume-specific *flux of a chemical reaction* r is the time derivative of the
929 advancement of the reaction per unit volume, $J_{V,B} = d_r\check{c}_B/dt \cdot V^{-1}$ [(mol·s⁻¹)·L⁻¹]. The *rate of*
930 *concentration change* is dc_B/dt [(mol·L⁻¹)·s⁻¹], where concentration is $c_B = n_B/V$. It is helpful to
931 make the subtle distinction between [mol·s⁻¹·L⁻¹] and [mol·L⁻¹·s⁻¹] for the fundamentally
932 different quantities of volume-specific flux and rate of concentration change, which merge to a
933 single expression only in closed systems. In open systems, external fluxes (such as O₂ supply)
934 are distinguished from internal transformations (metabolic flux, O₂ consumption). In a closed
935 system, external flows of all substances are zero and O₂ consumption (internal flow), I_{O_2}
936 [pmol·s⁻¹], causes a decline of the amount of O₂ in the system, n_{O_2} [nmol]. Normalization of
937 these quantities for the volume of the system, V [L = dm³], yields volume-specific O₂ flux, J_{V,O_2}
938 = I_{O_2}/V [nmol·s⁻¹·L⁻¹], and O₂ concentration, [O₂] or $c_{O_2} = n_{O_2}/V$ [nmol·mL⁻¹ = μmol·L⁻¹ = μM].
939 Instrumental background O₂ flux is due to external flux into a non-ideal closed respirometer,
940 such that total volume-specific flux has to be corrected for instrumental background O₂ flux,
941 *i.e.* O₂ diffusion into or out of the instrumental chamber. J_{V,O_2} is relevant mainly for
942 methodological reasons and should be compared with the accuracy of instrumental resolution
943 of background-corrected flux, *e.g.* ±1 nmol·s⁻¹·L⁻¹ (Gnaiger 2001). ‘Metabolic’ or catabolic
944 indicates O₂ flux, $J_{O_2,k}$, corrected for instrumental background O₂ flux and chemical background
945 O₂ flux due to autoxidation of chemical components added to the incubation medium.

946

947

948

949 4.2. System-specific and sample-specific normalization

950 Application of common and generally defined units is required for direct transfer of
 951 reported results into a database. The second [s] is the *SI* unit for the base quantity *time*. It is also
 952 the standard time-unit used in solution chemical kinetics. **Table 6** lists some conversion factors
 953 to obtain *SI* units. The term *rate* is not sufficiently defined to be useful for a database (**Fig. 7**).
 954 The inconsistency of the meanings of rate becomes fully apparent when considering Galileo
 955 Galilei's famous principle, that 'bodies of different weight all fall at the same rate (have a
 956 constant acceleration)' (Coopersmith 2010).

957 **Extensive quantities:** An extensive quantity increases proportionally with system size.
 958 The magnitude of an extensive quantity is completely additive for non-interacting subsystems,
 959 such as mass or flow expressed per defined system. The magnitude of these quantities depends
 960 on the extent or size of the system (Cohen *et al.* 2008).

961

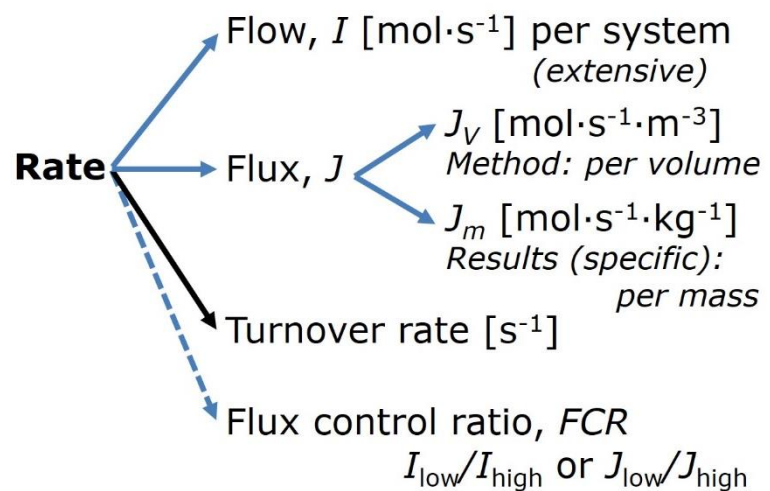
962 **Fig. 7. Different meanings of rate**

963 may lead to confusion, if the
 964 normalization is not sufficiently
 965 specified. Results are frequently
 966 expressed as mass-specific flux, J_m ,
 967 per mg protein, dry or wet weight
 968 (mass). Cell volume, V_{cell} , or
 969 mitochondrial volume, V_{mt} , may be
 970 used for normalization (volume-

971 specific flux, $J_{V_{\text{cell}}}$ or $J_{V_{\text{mt}}}$), which then must be clearly distinguished from flux, J_v , expressed for
 972 methodological reasons per volume of the measurement system, or flow per cell, I_x .

973

974 **Size-specific quantities:** 'The adjective *specific* before the name of an extensive quantity
 975 is often used to mean *divided by mass*' (Cohen *et al.* 2008). Mass-specific flux is flow divided
 976 by mass of the system. A mass-specific quantity is independent of the extent of non-interacting



977 homogenous subsystems. Tissue-specific quantities are of fundamental interest in comparative
 978 mitochondrial physiology, where *specific* refers to the *type* rather than *mass* of the tissue. The
 979 term *specific*, therefore, must be further clarified, such that tissue mass-specific, *e.g.*, muscle
 980 mass-specific quantities are defined.

981 **Molar quantities:** ‘The adjective *molar* before the name of an extensive quantity
 982 generally means *divided by amount of substance*’ (Cohen *et al.* 2008). The notion that all molar
 983 quantities then become *intensive* causes ambiguity in the meaning of *molar Gibbs energy*. It is
 984 important to emphasize the fundamental difference between normalization for amount of
 985 substance *in a system* or for amount of motive substance *in a transformation*. When the Gibbs
 986 energy of a system, G [J], is divided by the amount of substance B in the system, n_B [mol], a
 987 *size-specific* molar quantity is obtained, $G_B = G/n_B$ [J·mol⁻¹], which is not any force at all. In
 988 contrast, when the partial Gibbs energy change, $\partial_r G$ [J], is divided by the motive amount of
 989 substance B in reaction r (advancement of reaction), $\partial_r \xi_B$ [mol], the resulting intensive molar
 990 quantity, $F_{B,r} = \partial G / \partial_r \xi_B$ [J·mol⁻¹], is the chemical motive force of reaction r involving 1 mol B
 991 (**Table 5**, Note 4).

992 **Flow per system, I :** In analogy to electrical terms, flow as an extensive quantity (I ; per
 993 system) is distinguished from flux as a size-specific quantity (J ; per system size) (**Fig. 7**).
 994 Electric current is flow, I_{el} [A = C·s⁻¹] per system (extensive quantity). When dividing this
 995 extensive quantity by system size (membrane area), a size-specific quantity is obtained, which
 996 is electric flux (electric current density), J_{el} [A·m⁻² = C·s⁻¹·m⁻²].

997 **Size-specific flux, J :** Metabolic O₂ flow per tissue increases as tissue mass is increased.
 998 Tissue mass-specific O₂ flux should be independent of the size of the tissue sample studied in
 999 the instrument chamber, but volume-specific O₂ flux (per volume of the instrument chamber,
 1000 V) should increase in direct proportion to the amount of sample in the chamber. Accurate
 1001 definition of the experimental system is decisive: whether the experimental chamber is the
 1002 closed, open, isothermal or non-isothermal *system* with defined volume as part of the

1003 measurement apparatus, in contrast to the experimental *sample* in the chamber (**Table 6**).
1004 Volume-specific O₂ flux depends on mass-concentration of the sample in the chamber, but
1005 should be independent of the chamber volume. There are practical limitations to increasing the
1006 mass-concentration of the sample in the chamber, when one is concerned about crowding
1007 effects and instrumental time resolution.

1008 **Sample concentration C_{mX} :** Normalization for sample concentration is required for
1009 reporting respiratory data. Consider a tissue or cells as the sample, X , and the sample mass, m_X
1010 [mg] from which a mitochondrial preparation is obtained. The sample mass is frequently
1011 measured as wet or dry weight ($m_X \equiv W_w$ or W_d [mg]), or as amount of tissue or cell protein (m_X
1012 $\equiv m_{\text{Protein}}$). In the case of permeabilized tissues, cells, and homogenates, the sample
1013 concentration, $C_{mX} = m_X/V$ [$\text{mg}\cdot\text{mL}^{-1} = \text{g}\cdot\text{L}^{-1}$], is simply the mass of the subsample of tissue that
1014 is transferred into the instrument chamber. Part of the mitochondria from the tissue is lost during
1015 preparation of isolated mitochondria, and only a fraction of mitochondria is obtained, expressed
1016 as the mitochondrial yield (**Fig. 8**). At a high mitochondrial yield the sample of isolated
1017 mitochondria is more representative of the total mitochondrial population than in preparations
1018 characterized by low mitochondrial yield. Determination of the mitochondrial yield is based on
1019 measurement of the concentration of a mitochondrial marker in the tissue homogenate, $C_{\text{mte,thom}}$,
1020 which simultaneously provides information on the specific mitochondrial density in the sample
1021 (**Fig. 8**).

1022 Tissues can contain multiple cell populations which may have distinct mitochondrial
1023 subtypes. Mitochondria are also in a constant state of flux due to highly dynamic fission and
1024 fusion cycles, and can exist in multiple stages and sizes which may be altered by a range of
1025 factors. The isolation of mitochondria (often achieved through differential centrifugation) can
1026 therefore yield a subsample of the mitochondrial types present in a tissue, dependent on
1027 isolation protocols utilized (*e.g.* centrifugation speed). This possible artefact should be taken
1028 into account when planning experiments using isolated mitochondria. The tendency for

1029 mitochondria of specific sizes to be enriched at different centrifugation speeds also has the
 1030 potential to allow the isolation of specific mitochondrial subpopulations and therefore the
 1031 analysis of mitochondria from multiple cell lineages within a single tissue.

1032

1033 **Table 6. Sample concentrations and normalization of flux with SI/base units.**
 1034

Expression	Symbol	Definition	SI Unit	Notes
Sample				
Identity of sample	X	Cells, animals, patients		
Number of sample entities X	N_X	Number of cells, <i>etc.</i>	x	
Mass of sample X	m_X		kg	1
Mass of entity X	M_X	$M_X = m_X \cdot N_X^{-1}$	$\text{kg} \cdot \text{x}^{-1}$	1
Mitochondria				
Mitochondria	mt	$X = \text{mt}$		
Amount of mt-elements	mte	Quantity of mt-marker	x_{mte}	
Concentrations				
Sample number concentration	C_{NX}	$C_{NX} = N_X \cdot V^{-1}$	$\text{x} \cdot \text{m}^{-3}$	2
Sample mass concentration	C_{mX}	$C_{mX} = m_X \cdot V^{-1}$	$\text{kg} \cdot \text{m}^{-3}$	
Mitochondrial concentration	C_{mte}	$C_{\text{mte}} = \text{mte} \cdot V^{-1}$	$x_{\text{mte}} \cdot \text{m}^{-3}$	3
Specific mitochondrial density	D_{mte}	$D_{\text{mte}} = \text{mte} \cdot m_X^{-1}$	$x_{\text{mte}} \cdot \text{kg}^{-1}$	4
Mitochondrial content, mte per entity X	mte_X	$\text{mte}_X = \text{mte} \cdot N_X^{-1}$	$x_{\text{mte}} \cdot \text{x}^{-1}$	5
O₂ flow and flux				
Flow	I_{O_2}	Internal flow	$\text{mol} \cdot \text{s}^{-1}$	6
Volume-specific flux	J_{V,O_2}	$J_{V,\text{O}_2} = I_{\text{O}_2} \cdot V^{-1}$	$\text{mol} \cdot \text{s}^{-1} \cdot \text{m}^{-3}$	7
Flow per sample entity X	I_{X,O_2}	$I_{X,\text{O}_2} = J_{V,\text{O}_2} \cdot C_{NX}^{-1}$	$\text{mol} \cdot \text{s}^{-1} \cdot \text{x}^{-1}$	8
Mass-specific flux	J_{mX,O_2}	$J_{mX,\text{O}_2} = J_{V,\text{O}_2} \cdot C_{mX}^{-1}$	$\text{mol} \cdot \text{s}^{-1} \cdot \text{kg}^{-1}$	9
Mitochondria-specific flux	$J_{\text{mte},\text{O}_2}$	$J_{\text{mte},\text{O}_2} = J_{V,\text{O}_2} \cdot C_{\text{mte}}^{-1}$	$\text{mol} \cdot \text{s}^{-1} \cdot x_{\text{mte}}^{-1}$	10

1035

1036 1 The SI prefix k is used for the SI base unit of mass (kg = 1,000 g). In praxis, various SI prefixes are
 1037 used for convenience, to make numbers easily readable, e.g. 1 mg tissue, cell or mitochondrial mass
 1038 instead of 0.000001 kg.

1039 2 In case $X = \text{cells}$, the sample number concentration is $C_{N_{\text{cell}}} = N_{\text{cell}} \cdot V^{-1}$, and volume may be expressed
 1040 in [$\text{dm}^3 = \text{L}$] or [$\text{cm}^3 = \text{mL}$]. See **Table 7** for different sample types.

1041 3 mt-concentration is an experimental variable, dependent on sample concentration: (1) $C_{\text{mte}} = \text{mte} \cdot V^{-1}$;
 1042 (2) $C_{\text{mte}} = \text{mte}_X \cdot C_{NX}$; (3) $C_{\text{mte}} = C_{mX} \cdot D_{\text{mte}}$.

1043 4 If the amount of mitochondria, mte, is expressed as mitochondrial mass, then D_{mte} is the mass
 1044 fraction of mitochondria in the sample. If mte is expressed as mitochondrial volume, V_{mt} , and the

1045 mass of sample, m_X , is replaced by volume of sample, V_X , then D_{mte} is the volume fraction of
1046 mitochondria in the sample.

1047 5 $mte_X = mte \cdot N_X^{-1} = C_{mte} \cdot C_{NX}^{-1}$.

1048 6 Entity O_2 can be replaced by other chemical entities B to study different reactions.

1049 7 I_{O_2} and V are defined per instrument chamber as a system of constant volume (and constant
1050 temperature), which may be closed or open. I_{O_2} is abbreviated for $I_{O_2,r}$, *i.e.* the metabolic or internal
1051 O_2 flow of the chemical reaction r in which O_2 is consumed, hence the negative stoichiometric
1052 number, $\nu_{O_2} = -1$. $I_{O_2,r} = d_r n_{O_2} / dt \cdot \nu_{O_2}^{-1}$. If r includes all chemical reactions in which O_2 participates,
1053 then $d_r n_{O_2} = dn_{O_2} - d_e n_{O_2}$, where dn_{O_2} is the change in the amount of O_2 in the instrument chamber
1054 and $d_e n_{O_2}$ is the amount of O_2 added externally to the system. At steady state, by definition $dn_{O_2} = 0$,
1055 hence $d_r n_{O_2} = -d_e n_{O_2}$.

1056 8 J_{V,O_2} is an experimental variable, expressed per volume of the instrument chamber.

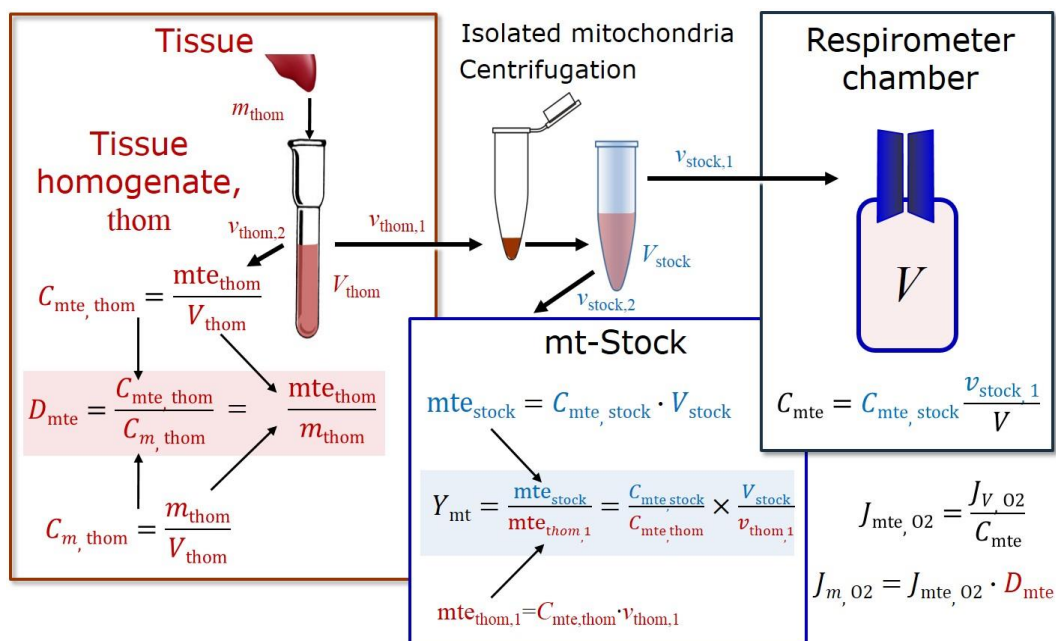
1057 9 I_{X,O_2} is a physiological variable, depending on the size of entity X .

1058 10 There are many ways to normalize for a mitochondrial marker, that are used in different experimental
1059 approaches: (1) $J_{mte,O_2} = J_{V,O_2} \cdot C_{mte}^{-1}$; (2) $J_{mte,O_2} = J_{V,O_2} \cdot C_{mX}^{-1} \cdot D_{mte}^{-1} = J_{mX,O_2} \cdot D_{mte}^{-1}$; (3) $J_{mte,O_2} =$
1060 $J_{V,O_2} \cdot C_{mX}^{-1} \cdot mte_X^{-1} = I_{X,O_2} \cdot mte_X^{-1}$; (4) $J_{mte,O_2} = I_{O_2} \cdot mte^{-1}$.

1061

1062 **Mass-specific flux, J_{mX,O_2} :** Mass-specific flux is obtained by expressing respiration per
1063 mass of sample, m_X [mg]. X is the type of sample, *e.g.*, tissue homogenate, permeabilized fibres
1064 or cells. Volume-specific flux is divided by mass concentration of X , $J_{mX,O_2} = J_{V,O_2} / C_{mX}$; or flow
1065 per cell is divided by mass per cell, $J_{mcell,O_2} = I_{cell,O_2} / M_{cell}$. If mass-specific O_2 flux is constant
1066 and independent of sample size (expressed as mass), then there is no interaction between the
1067 subsystems. A 1.5 mg and a 3.0 mg muscle sample respire at identical mass-specific flux.
1068 Mass-specific O_2 flux, however, may change with the mass of a tissue sample, cells or isolated
1069 mitochondria in the measuring chamber, in which case the nature of the interaction becomes an
1070 issue. Optimization of cell density and arrangement is generally important and particularly in
1071 experiments carried out in wells, considering the confluency of the cell monolayer or clumps
1072 of cells (Salabei *et al.* 2014).

1073



1074

Symbol	Definition [Units]
C_{mte}	Mitochondrial concentration in chamber [$x_{mte} \cdot L^{-1}$]
C_m	Sample mass concentration in chamber [$g \cdot L^{-1}$]
D_{mte}	Specific mte-density per tissue mass [$x_{mte} \cdot g^{-1}$]
J_{m,O_2}	Mass-specific O_2 flux [$nmol \cdot s^{-1} \cdot g^{-1}$]
J_{mte,O_2}	Mitochondria-specific O_2 flux [$nmol \cdot s^{-1} \cdot x_{mte}^{-1}$]
mte	Amount of mitochondrial elements [x_{mte}]
m_{thom}	Mass of tissue in the homogenate [g]
Y_{mt}	Yield of isolated mitochondria

1075

1076

1077

1078

1079

1080

1081

1082

1083

1084

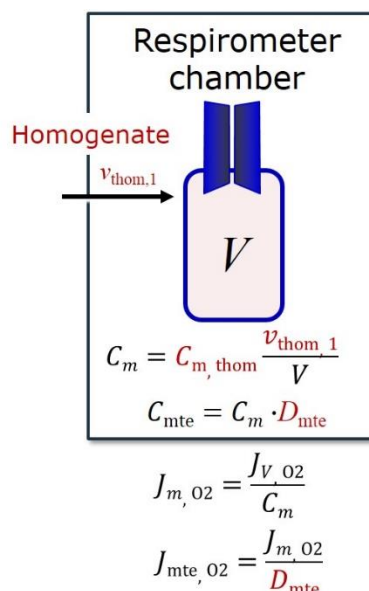


Fig. 8. Normalization of volume-specific flux of isolated mitochondria and tissue homogenate. A: Mitochondrial yield, Y_{mt} , in preparation of isolated mitochondria. $v_{thom,1}$ and $v_{stock,1}$ are the volumes transferred from the total volume, V_{thom} and V_{stock} , respectively. $mte_{thom,1}$ is the amount of mitochondrial elements in volume $v_{thom,1}$ used for isolation. **B:** In respirometry with homogenate, $v_{thom,1}$ is transferred directly into the respirometer chamber. See **Table 6** for further explanation of symbols.

1085
1086

Table 7. Some useful abbreviations of various sample types, X.

Identity of sample	X
Mitochondrial preparation	mtprep
Isolated mitochondria	imt
Tissue homogenate	thom
Permeabilized tissue	pti
Permeabilized fibre	pfi
Permeabilized cell	pce
Cell	ce
Organism	org

1087

1088 **Number concentration, C_{NX} :** The experimental *number concentration* of sample in the
1089 case of cells or animals, *e.g.*, nematodes is $C_{NX} = N_X/V$ [$x \cdot \text{mL}^{-1}$], where N_X is the number of
1090 cells or organisms in the chamber (**Table 6**).

1091 **Flow per sample entity, I_{X,O_2} :** A special case of normalization is encountered in
1092 respiratory studies with permeabilized (or intact) cells. If respiration is expressed per cell, the
1093 O_2 flow per measurement system is replaced by the O_2 flow per cell, I_{cell,O_2} (**Table 6**). O_2 flow
1094 can be calculated from volume-specific O_2 flux, J_{V,O_2} [$\text{nmol} \cdot \text{s}^{-1} \cdot \text{L}^{-1}$] (per V of the measurement
1095 chamber [L]), divided by the number concentration of cells, $C_{N_{ce}} = N_{ce}/V$ [$\text{cell} \cdot \text{L}^{-1}$], where N_{ce}
1096 is the number of cells in the chamber. Cellular O_2 flow can be compared between cells of
1097 identical size. To take into account changes and differences in cell size, further normalization
1098 is required to obtain cell size-specific or mitochondrial marker-specific O_2 flux (Renner *et al.*
1099 2003).

1100 The complexity changes when the sample is a whole organism studied as an experimental
1101 model. The well-established scaling law in respiratory physiology reveals a strong interaction
1102 of O_2 consumption and individual body mass of an organism, since *basal* metabolic rate (flow)
1103 does not increase linearly with body mass, whereas *maximum* mass-specific O_2 flux, $\dot{V}_{O_2\text{max}}$ or

1104 $\dot{V}_{O_{2peak}}$, is approximately constant across a large range of individual body mass (Weibel and
1105 Hoppeler 2005), with individuals, breeds, and certain species deviating substantially from this
1106 general relationship. $\dot{V}_{O_{2peak}}$ of human endurance athletes is 60 to 80 mL O₂·min⁻¹·kg⁻¹ body
1107 mass, converted to $J_{m,O_{2peak}}$ of 45 to 60 nmol·s⁻¹·g⁻¹ (Gnaiger 2014; **Table 8**).

1108

1109 *4.3. Normalization for mitochondrial content*

1110 Normalization is a problematic subject and it is essential to consider the question of the
1111 study. If the study aims to compare tissue performance, such as the effects of a certain treatment
1112 on a specific tissue, then normalization can be successful, using tissue mass or protein content,
1113 for example. If the aim, however, is to find differences of mitochondrial function independent
1114 of mitochondrial density (**Table 6**), then normalization to a mitochondrial marker is imperative
1115 (**Fig. 9**). However, one cannot assume that quantitative changes in various markers such as
1116 mitochondrial proteins necessarily occur in parallel with one another. It is important to first
1117 establish that the marker chosen is not selectively altered by the performed treatment. In
1118 conclusion, the normalization must reflect the question under investigation to reach a satisfying
1119 answer. On the other hand, the goal of comparing results across projects and institutions
1120 requires some standardization on normalization for entry into a databank.

1121 **Mitochondrial concentration, C_{mte} , and mitochondrial markers:** It is important that
1122 mitochondrial concentration in the tissue and the measurement chamber be quantified, as a
1123 physiological output and result of mitochondrial biogenesis and degradation, and as a quantity
1124 for normalization in functional analyses. Mitochondrial organelles comprise a cellular
1125 reticulum that is in a continual flux of fusion and fission. Hence the definition of an "amount"
1126 of mitochondria is often misconceived: mitochondria cannot be counted as a number of
1127 occurring elements. Therefore, quantification of the "amount" of mitochondria depends on
1128 measurement of chosen mitochondrial markers. 'Mitochondria are the structural and functional
1129 elemental units of cell respiration' (Gnaiger 2014). The quantity of a mitochondrial marker can

1130 be considered as the measurement of the amount of *elemental mitochondrial units* or
 1131 *mitochondrial elements*, mte. However, since mitochondrial quality changes under certain
 1132 stimuli, particularly in mitochondrial dysfunction and after exercise training (Pesta *et al.* 2011;
 1133 Campos *et al.* 2017), some markers can vary while other markers are unchanged. (1)
 1134 Mitochondrial volume and membrane area are structural markers, whereas mitochondrial
 1135 protein mass is frequently used as a marker for isolated mitochondria. (2) Molecular and
 1136 enzymatic mitochondrial markers (amounts or activities) can be selected as matrix markers,
 1137 *e.g.*, citrate synthase activity, mtDNA; or inner mt-membrane markers, *e.g.*, cytochrome *c*
 1138 oxidase activity, *aa*₃ content, cardiolipin, TOM20. (3) Extending the measurement of
 1139 mitochondrial marker enzyme activity to mitochondrial pathway capacity, measured as ET or
 1140 OXPHOS capacity, can be considered as an integrative functional mitochondrial marker.

1141 Depending on the type of mitochondrial marker, the mitochondrial elements, mte, are
 1142 expressed in marker-specific units. Although concentration and density are used synonymously
 1143 in physical chemistry, it is recommended to distinguish *experimental mitochondrial*
 1144 *concentration*, $C_{\text{mte}} = \text{mte}/V$ and *physiological mitochondrial density*, $D_{\text{mte}} = \text{mte}/m_X$. Then
 1145 mitochondrial density is the amount of mitochondrial elements per mass of tissue (**Fig. 9**). The
 1146 former is mitochondrial density multiplied by sample mass concentration, $C_{\text{mte}} = D_{\text{mte}} \cdot C_{mX}$, or
 1147 mitochondrial content multiplied by sample number concentration, $C_{\text{mte}} = \text{mte}_X \cdot C_{NX}$ (**Table 6**).

1148 **Mitochondria-specific flux, $J_{\text{mte},\text{O}_2}$:** Volume-specific metabolic O₂ flux depends on: (1)
 1149 the sample concentration in the volume of the instrument chamber, C_{mX} , or C_{NX} ; (2) the
 1150 mitochondrial density in the sample, $D_{\text{mte}} = \text{mte}/m_X$ or $\text{mte}_X = \text{mte}/N_X$; and (3) the specific
 1151 mitochondrial activity or performance per elemental mitochondrial unit, $J_{\text{mte},\text{O}_2} = J_{V,\text{O}_2}/C_{\text{mte}}$
 1152 (**Table 6**). Obviously, the numerical results for $J_{\text{mte},\text{O}_2}$ vary according to the type of
 1153 mitochondrial marker chosen for measurement of mte and $C_{\text{mte}} = \text{mte}/V$.

Flow, Performance	=	Element function	x	Element density	x	Size of entity
$\frac{\text{mol}\cdot\text{s}^{-1}}{X}$	=	$\frac{\text{mol}\cdot\text{s}^{-1}}{X_{\text{mte}}}$	·	$\frac{X_{\text{mte}}}{\text{kg}}$	·	$\frac{\text{kg}}{X}$

A	Flow	=	mt-specific flux	x	mt-structure, functional elements
	I_{X,O_2}	=	J_{mte,O_2}	·	mte_X
					$\left(\frac{\text{mte}_X}{M_X} \cdot M_X \right)$

I_{X,O_2}	=	J_{mte,O_2}	·	D_{mte}	·	M_X
$\frac{I_{X,O_2}}{M_X}$	=	$\frac{I_{X,O_2}}{\text{mte}_X}$	·	$\frac{\text{mte}_X}{M_X}$		

B	I_{X,O_2}	=	J_{mX,O_2}	·	M_X
	Flow	=	Entity mass-specific flux	x	Mass of entity

1154
1155 **Fig. 9. Structure-function analysis of performance of an**
1156 **organism, organ or tissue, or a cell (sample entity X). O₂**
1157 **flow, I_{X,O_2} , is the product of performance per functional**
1158 **element (element function, mitochondria-specific flux),**
1159 **element density (mitochondrial density, D_{mte}), and size of**
1160 **entity X (mass M_X). (A) Structured analysis: performance is the**
1161 **product of mitochondrial *function* (mt-specific flux) and *structure***
1162 **(functional elements; D_{mte} times mass of X). (B) Unstructured**
1163 **analysis: performance is the product of *entity mass-specific flux*,**
1164 **$J_{mX,O_2} = I_{X,O_2}/M_X = I_{O_2}/m_X$ [mol·s⁻¹·kg⁻¹] and *size of entity*,**
1165 **expressed as mass of X; $M_X = m_X \cdot N_X^{-1}$ [kg·x⁻¹]. See Table 6 for**
1166 **further explanation of quantities and units. Modified from Gnaiger**
1167 **(2014).**

1168 4.4. Evaluation of mitochondrial markers

1170 Different methods are implicated in quantification of mitochondrial markers and have
1171 different strengths. Some problems are common for all mitochondrial markers, mte: (I)
1172 Accuracy of measurement is crucial, since even a highly accurate and reproducible

1173 measurement of O₂ flux results in an inaccurate and noisy expression normalized for a biased
1174 and noisy measurement of a mitochondrial marker. This problem is acute in mitochondrial
1175 respiration because the denominators used (the mitochondrial markers) are often very small
1176 moieties whose accurate and precise determination is difficult. This problem can be avoided
1177 when O₂ fluxes measured in substrate-uncoupler-inhibitor titration protocols are normalized for
1178 flux in a defined respiratory reference state, which is used as an *internal* marker and yields flux
1179 control ratios, *FCRs* (Fig. 7). *FCRs* are independent of any *externally* measured markers and,
1180 therefore, are statistically very robust, considering the limitations of ratios in general (Jasienski
1181 and Bazzaz 1999). *FCRs* indicate qualitative changes of mitochondrial respiratory control, with
1182 highest quantitative resolution, separating the effect of mitochondrial density or concentration
1183 on J_{mX,O_2} and I_{X,O_2} from that of function per elemental mitochondrial marker, J_{mte,O_2} (Pesta *et*
1184 *al.* 2011; Gnaiger 2014). (2) If mitochondrial quality does not change and only the amount of
1185 mitochondria, defined by the chosen mitochondrial marker, varies as a determinant of mass-
1186 specific flux, any marker is equally qualified in principle; then in practice selection of the
1187 optimum marker depends only on the accuracy and precision of measurement of the
1188 mitochondrial marker. (3) If mitochondrial flux control ratios change, then there may not be
1189 any best mitochondrial marker. In general, measurement of multiple mitochondrial markers
1190 enables a comparison and evaluation of normalization for a variety of mitochondrial markers.
1191 Evaluation of mitochondrial markers in healthy controls is insufficient for providing guidelines
1192 for application in the diagnosis of pathological states and specific treatments.

1193 In line with the concept of the respiratory control ratio (Chance and Williams 1955a), the
1194 most readily used normalization is that of flux control ratios and flux control factors (Gnaiger
1195 2014). Selection of the state of maximum flux in a protocol as the reference state has the
1196 advantages of (1) internal normalization, (2) statistical linearization of the response in the range
1197 of 0 to 1, and (3) consideration of maximum flux for integrating a very large number of
1198 elemental steps in the OXPHOS or ET-pathways. This reduces the risk of selecting a functional

1199 marker that is specifically altered by the treatment or pathodology, yet increases the chance that
1200 the highly integrative pathway is disproportionately affected, *e.g.* the OXPPOS rather than ET
1201 pathway in case of an enzymatic defect in the phosphorylation pathway. In this case, additional
1202 information can be obtained by reporting flux control ratios based on a reference state which
1203 indicates stable tissue-mass specific flux. Stereological determination of mitochondrial content
1204 via two-dimensional transmission electron microscopy can have limitations due to the dynamics
1205 of mitochondrial size (Meinild Lundby *et al.* 2017). Accurate determination of three-
1206 dimensional volume by two-dimensional microscopy can be both time consuming and
1207 statistically challenging (Larsen *et al.* 2012). Using mitochondrial marker enzymes (citrate
1208 synthase activity, Complex I–IV amount or activity) for normalization of flux is limited in part
1209 by the same factors that apply to the use of flux control ratios. Strong correlations between
1210 various mitochondrial markers and citrate synthase activity (Reichmann *et al.* 1985; Boushel *et*
1211 *al.* 2007; Mogensen *et al.* 2007) are expected in a specific tissue of healthy subjects and in
1212 disease states not specifically targeting citrate synthase. Citrate synthase activity is acutely
1213 modifiable by exercise (Tonkonogi *et al.* 1997; Leek *et al.* 2001). Evaluation of mitochondrial
1214 markers related to a selected age and sex cohort cannot be extrapolated to provide
1215 recommendations for normalization in respirometric diagnosis of disease, in different states of
1216 development and ageing, different cell types, tissues, and species. mtDNA normalised to nDNA
1217 via qPCR is correlated to functional mitochondrial markers including OXPPOS and ET
1218 capacity in some cases (Puntschart *et al.* 1995; Wang *et al.* 1999; Menshikova *et al.* 2006;
1219 Boushel *et al.* 2007), but lack of such correlations have been reported (Menshikova *et al.* 2005;
1220 Schultz and Wiesner 2000; Pesta *et al.* 2011). Several studies indicate a strong correlation
1221 between cardiolipin content and increase in mitochondrial functionality with exercise
1222 (Menshikova *et al.* 2005; Menshikova *et al.* 2007; Larsen *et al.* 2012; Faber *et al.* 2014), but its
1223 use as a general mitochondrial biomarker in disease remains questionable.

1224

1225 4.5. Conversion: units and normalization

1226 Many different units have been used to report the rate of oxygen consumption, OCR
1227 (**Table 8**). *SI* base units provide the common reference for introducing the theoretical principles
1228 (**Fig. 7**), and are used with appropriately chosen *SI* prefixes to express numerical data in the
1229 most practical format, with an effort towards unification within specific areas of application
1230 (**Table 9**). For studies of cells, we recommend that respiration be expressed, as far as possible,
1231 as (1) O₂ flux normalized for a mitochondrial marker, for separation of the effects of
1232 mitochondrial quality and content on cell respiration (this includes *FCRs* as a normalization for
1233 a functional mitochondrial marker); (2) O₂ flux in units of cell volume or mass, for comparison
1234 of respiration of cells with different cell size (Renner *et al.* 2003) and with studies on tissue
1235 preparations, and (3) O₂ flow in units of attomole (10⁻¹⁸ mol) of O₂ consumed by each cell in a
1236 second [amol·s⁻¹·cell⁻¹], numerically equivalent to [pmol·s⁻¹·10⁻⁶ cells]. This convention allows
1237 information to be easily used when designing experiments in which oxygen consumption must
1238 be considered. For example, to estimate the volume-specific O₂ flux in an instrument chamber
1239 that would be expected at a particular cell number concentration, one simply needs to multiply
1240 the flow per cell by the number of cells per volume of interest. This provides the amount of O₂
1241 [mol] consumed per time [s⁻¹] per unit volume [L⁻¹]. At an O₂ flow of 100 amol·s⁻¹·cell⁻¹ and a
1242 cell density of 10⁹ cells·L⁻¹ (10⁶ cells·mL⁻¹), the volume-specific O₂ flux is 100 nmol·s⁻¹·L⁻¹ (100
1243 pmol·s⁻¹·mL⁻¹).

1244 Although volume is expressed as m³ using the *SI* base unit, the litre [dm³] is the basic unit
1245 of volume for concentration and is used for most solution chemical kinetics. If one multiplies
1246 $I_{\text{cell},\text{O}_2}$ by C_{Ncell} , then the result will not only be the amount of O₂ [mol] consumed per time [s⁻¹]
1247 in one litre [L⁻¹], but also the change in the concentration of oxygen per second (for any volume
1248 of an ideally closed system). This is ideal for kinetic modeling as it blends with chemical rate
1249 equations where concentrations are typically expressed in mol·L⁻¹ (Wagner *et al.* 2011). In
1250 studies of multinuclear cells, such as differentiated skeletal muscle cells, it is easy to determine

1251 the number of nuclei but not the total number of cells. A generalized concept, therefore, is
 1252 obtained by substituting cells by nuclei as the sample entity. This does not hold, however, for
 1253 enucleated platelets.

1254

1255 **Table 8. Conversion of various units used in respirometry and**
 1256 **ergometry.** e is the number of electrons or reducing equivalents. z_B is the
 1257 charge number of entity B.

1258

1 Unit	x	Multiplication factor	SI-Unit	Note
ng.atom O \cdot s $^{-1}$	(2 e)	0.5	nmol O $_2$ \cdot s $^{-1}$	
ng.atom O \cdot min $^{-1}$	(2 e)	8.33	pmol O $_2$ \cdot s $^{-1}$	
natom O \cdot min $^{-1}$	(2 e)	8.33	pmol O $_2$ \cdot s $^{-1}$	
nmol O $_2$ \cdot min $^{-1}$	(4 e)	16.67	pmol O $_2$ \cdot s $^{-1}$	
nmol O $_2$ \cdot h $^{-1}$	(4 e)	0.2778	pmol O $_2$ \cdot s $^{-1}$	
mL O $_2$ \cdot min $^{-1}$ at STPD ^a		0.744	μ mol O $_2$ \cdot s $^{-1}$	1
W = J/s at -470 kJ/mol O $_2$		-2.128	μ mol O $_2$ \cdot s $^{-1}$	
mA = mC \cdot s $^{-1}$	($z_{H^+} = 1$)	10.36	nmol H $^+$ \cdot s $^{-1}$	2
mA = mC \cdot s $^{-1}$	($z_{O_2} = 4$)	2.59	nmol O $_2$ \cdot s $^{-1}$	2
nmol H $^+$ \cdot s $^{-1}$	($z_{H^+} = 1$)	0.09649	mA	3
nmol O $_2$ \cdot s $^{-1}$	($z_{O_2} = 4$)	0.38594	mA	3

1259

1260 1 At standard temperature and pressure dry (STPD: 0 °C = 273.15 K and 1 atm =
 1261 101.325 kPa = 760 mmHg), the molar volume of an ideal gas, V_m , and V_{m,O_2} is
 1262 22.414 and 22.392 L \cdot mol $^{-1}$ respectively. Rounded to three decimal places, both
 1263 values yield the conversion factor of 0.744. For comparison at NTPD (20 °C),
 1264 V_{m,O_2} is 24.038 L \cdot mol $^{-1}$. Note that the SI standard pressure is 100 kPa.

1265 2 The multiplication factor is $10^6/(z_B \cdot F)$.

1266 3 The multiplication factor is $z_B \cdot F/10^6$.

1267

1268 4.5. Conversion: oxygen, proton and ATP flux

1269 $J_{O_2,k}$ is coupled in mitochondrial steady states to proton cycling, $J_{\infty H^+} = J_{H^+,out} = J_{H^+,in}$
 1270 (**Fig. 2**). $J_{H^+,out/n}$ and $J_{H^+,in/n}$ [$\text{nmol}\cdot\text{s}^{-1}\cdot\text{L}^{-1}$] are converted into electrical units, $J_{H^+,out/e}$ [$\text{mC}\cdot\text{s}^{-1}\cdot\text{L}^{-1}$
 1271 $= \text{mA}\cdot\text{L}^{-1}$] = $J_{H^+,out/n}$ [$\text{nmol}\cdot\text{s}^{-1}\cdot\text{L}^{-1}$] $\cdot F$ [$\text{C}\cdot\text{mol}^{-1}$] $\cdot 10^{-6}$ (**Table 4**). At a $J_{H^+,out}/J_{O_2,k}$ ratio or H^+_{out}/O_2
 1272 of 20 ($H^+_{out}/O = 10$), a volume-specific O_2 flux of $100 \text{ nmol}\cdot\text{s}^{-1}\cdot\text{L}^{-1}$ would correspond to a proton
 1273 flux of $2,000 \text{ nmol H}^+_{out}\cdot\text{s}^{-1}\cdot\text{L}^{-1}$ or volume-specific current of $193 \text{ mA}\cdot\text{L}^{-1}$.

$$1274 \quad J_{V,H^+out/e} [\text{mA}\cdot\text{L}^{-1}] = J_{V,H^+out/n} \cdot F \cdot 10^{-6} [\text{nmol}\cdot\text{s}^{-1}\cdot\text{L}^{-1} \cdot \text{mC}\cdot\text{nmol}^{-1}] \quad (\text{Eq. 3.1})$$

$$1275 \quad J_{V,H^+out/e} [\text{mA}\cdot\text{L}^{-1}] = J_{V,O_2} \cdot (H^+_{out}/O_2) \cdot F \cdot 10^{-6} [\text{mC}\cdot\text{s}^{-1}\cdot\text{L}^{-1} = \text{mA}\cdot\text{L}^{-1}] \quad (\text{Eq. 3.2})$$

1276

1277 **Table 9. Conversion of units with preservation of numerical values.**

Name	Frequently used unit	Equivalent unit	Note
Volume-specific flux, J_{V,O_2}	$\text{pmol}\cdot\text{s}^{-1}\cdot\text{mL}^{-1}$	$\text{nmol}\cdot\text{s}^{-1}\cdot\text{L}^{-1}$	1
	$\text{mmol}\cdot\text{s}^{-1}\cdot\text{L}^{-1}$	$\text{mol}\cdot\text{s}^{-1}\cdot\text{m}^{-3}$	
Cell-specific flow, I_{O_2}	$\text{pmol}\cdot\text{s}^{-1}\cdot 10^{-6} \text{ cells}$	$\text{amol}\cdot\text{s}^{-1}\cdot\text{cell}^{-1}$	2
	$\text{pmol}\cdot\text{s}^{-1}\cdot 10^{-9} \text{ cells}$	$\text{zmol}\cdot\text{s}^{-1}\cdot\text{cell}^{-1}$	
Cell number concentration, C_{Nce}	$10^6 \text{ cells}\cdot\text{mL}^{-1}$	$10^9 \text{ cells}\cdot\text{L}^{-1}$	
Mitochondrial protein concentration, C_{mte}	$0.1 \text{ mg}\cdot\text{mL}^{-1}$	$0.1 \text{ g}\cdot\text{L}^{-1}$	
Mass-specific flux, J_{m,O_2}	$\text{pmol}\cdot\text{s}^{-1}\cdot\text{mg}^{-1}$	$\text{nmol}\cdot\text{s}^{-1}\cdot\text{g}^{-1}$	4
Catabolic power, $P_{O_2,k}$	$\mu\text{W}\cdot 10^{-6} \text{ cells}$	$\text{pW}\cdot\text{cell}^{-1}$	1
Volume	1,000 L	m^3 (1,000 kg)	
	L	dm^3 (kg)	
	mL	cm^3 (g)	
	μL	mm^3 (mg)	
	fL	μm^3 (pg)	
Amount of substance concentration	$\text{M} = \text{mol}\cdot\text{L}^{-1}$	$\text{mol}\cdot\text{dm}^{-3}$	

1278

1279 1 pmol: picomole = 10^{-12} mol1280 2 amol: attomole = 10^{-18} mol1281 3 zmol: zeptomole = 10^{-21} mol1282 4 nmol: nanomole = 10^{-9} mol

1283

1284 ET capacity in various human cell types including HEK 293, primary HUVEC and fibroblasts
 1285 ranges from 50 to $180 \text{ amol}\cdot\text{s}^{-1}\cdot\text{cell}^{-1}$, measured in intact cells in the noncoupled state (see
 1286 Gnaiger 2014). At $100 \text{ amol}\cdot\text{s}^{-1}\cdot\text{cell}^{-1}$ corrected for ROX (corresponding to a catabolic power
 1287 of $-48 \text{ pW}\cdot\text{cell}^{-1}$), the current across the mt-membranes, I_e , approximates $193 \text{ pA}\cdot\text{cell}^{-1}$ or 0.2

1288 nA per cell. See Rich (2003) for an extension of quantitative bioenergetics from the molecular
 1289 to the human scale, with a transmembrane proton flux equivalent to 520 A in an adult at a
 1290 catabolic power of -110 W. Modelling approaches illustrate the link between proton motive
 1291 force and currents (Willis *et al.* 2016). For NADH- and succinate-linked respiration, the
 1292 mechanistic P_{\gg}/O_2 ratio (referring to the full 4 electron reduction of O_2) is calculated at 20/3.7
 1293 and 12/3.7, respectively (Eq. 4) equal to 5.4 and 3.3. The classical P_{\gg}/O ratios (referring to the
 1294 2 electron reduction of 0.5 O_2) are 2.7 and 1.6 (Watt *et al.* 2010), in direct agreement with the
 1295 measured P_{\gg}/O ratio for succinate of 1.58 ± 0.02 (Gnaiger *et al.* 2000; for detailed reviews see
 1296 Wikström and Hummer 2012; Sazanov 2015),

$$1297 \quad P_{\gg}/O_2 = (H^+_{out}/O_2)/(H^+_{in}/P_{\gg}) \quad (\text{Eq. 4})$$

1298 In summary (**Fig. 1**),

$$1299 \quad J_{V,P_{\gg}} [\text{nmol}\cdot\text{s}^{-1}\cdot\text{L}^{-1}] = J_{V,O_2} \cdot (H^+_{out}/O_2)/(H^+_{in}/P_{\gg}) \quad (\text{Eq. 5.1})$$

$$1300 \quad J_{V,P_{\gg}} [\text{nmol}\cdot\text{s}^{-1}\cdot\text{L}^{-1}] = J_{V,O_2} \cdot (P_{\gg}/O_2) \quad (\text{Eq. 5.2})$$

1301 We consider isolated mitochondria as powerhouses and proton pumps as molecular machines
 1302 to relate experimental results to energy metabolism of the intact cell. The cellular P_{\gg}/O_2 based
 1303 on oxidation of glycogen is increased by the glycolytic (fermentative) substrate-level
 1304 phosphorylation of 3 P_{\gg}/Glyc , *i.e.*, 0.5 mol P_{\gg} for each mol O_2 consumed in the complete
 1305 oxidation of a mol glycosyl unit (Glyc). Adding 0.5 to the mitochondrial P_{\gg}/O_2 ratio of 5.4
 1306 yields a bioenergetic cell physiological P_{\gg}/O_2 ratio close to 6. Two NADH equivalents are
 1307 formed during glycolysis and transported from the cytosol into the mitochondrial matrix, either
 1308 by the malate-aspartate shuttle or by the glycerophosphate shuttle resulting in different
 1309 theoretical yield of ATP generated by mitochondria, the energetic cost of which potentially
 1310 must be taken into account. Considering also substrate-level phosphorylation in the TCA cycle,
 1311 this high P_{\gg}/O_2 ratio not only reflects proton translocation and OXPHOS studied in isolation,
 1312 but integrates mitochondrial physiology with energy transformation in the living cell (Gnaiger
 1313 1993a).

1314

1315 **5. Conclusions**

1316 MitoEAGLE can serve as a gateway to better diagnose mitochondrial respiratory defects
1317 linked to genetic variation, age-related health risks, sex-specific mitochondrial performance,
1318 lifestyle with its effects on degenerative diseases, and thermal and chemical environment. The
1319 present recommendations on coupling control states and rates, linked to the concept of the
1320 protonmotive force (Part 1) will be extended in a series of reports on pathway control of
1321 mitochondrial respiration, respiratory states in intact cells, and harmonization of experimental
1322 procedures.

1323

1324 Box 5: Mitochondrial and cell respiration

1325 Mitochondrial and cell respiration is the process of highly exergonic and exothermic energy
1326 transformation in which scalar redox reactions are coupled to vectorial ion translocation across
1327 a semipermeable membrane, which separates the small volume of a bacterial cell or
1328 mitochondrion from the larger volume of its surroundings. The electrochemical exergy can be
1329 partially conserved in the phosphorylation of ADP to ATP or in ion pumping, or dissipated in
1330 an electrochemical short-circuit. Respiration is thus clearly distinguished from fermentation as
1331 the counterpart of cellular core energy metabolism. Respiration is separated in mitochondrial
1332 preparations from the partial contribution of fermentative pathways of the intact cell. According
1333 to this definition, residual oxygen consumption, as measured after inhibition of mitochondrial
1334 electron transfer, does not belong to the class of catabolic reactions and is, therefore, subtracted
1335 from total oxygen consumption to obtain baseline-corrected respiration.

1336

1337 The optimal choice for expressing mitochondrial and cell respiration (**Box 5**) as O₂ flow
1338 per biological system, and normalization for specific tissue-markers (volume, mass, protein)
1339 and mitochondrial markers (volume, protein, content, mtDNA, activity of marker enzymes,

1340 respiratory reference state) is guided by the scientific question under study. Interpretation of
1341 the obtained data depends critically on appropriate normalization, and therefore reporting rates
1342 merely as $\text{nmol}\cdot\text{s}^{-1}$ is discouraged, since it restricts the analysis to intra-experimental
1343 comparison of relative (qualitative) differences. Expressing O_2 consumption per cell may not
1344 be possible when dealing with tissues. For studies with mitochondrial preparations, we
1345 recommend that normalizations be provided as far as possible: (1) on a per cell basis as O_2 flow
1346 (a biophysical normalization); (2) per g cell or tissue protein, or per cell or tissue mass as mass-
1347 specific O_2 flux (a cellular normalization); and (3) per mitochondrial marker as mt-specific flux
1348 (a mitochondrial normalization). With information on cell size and the use of multiple
1349 normalizations, maximum potential information is available (Renner *et al.* 2003; Wagner *et al.*
1350 2011; Gnaiger 2014). When using isolated mitochondria, mitochondrial protein is a frequently
1351 applied mitochondrial marker, the use of which is basically restricted to isolated mitochondria.
1352 Mitochondrial markers, such as citrate synthase activity as an enzymatic matrix marker, provide
1353 a link to the tissue of origin on the basis of calculating the mitochondrial yield, *i.e.*, the fraction
1354 of mitochondrial marker obtained from a unit mass of tissue.

1355

1356 **Acknowledgements**

1357 We thank M. Beno for management assistance. Supported by COST Action CA15203
1358 MitoEAGLE and K-Regio project MitoFit (EG).

1359 **Competing financial interests:** E.G. is founder and CEO of Oroboros Instruments, Innsbruck,
1360 Austria.

1361

1362 **6. References** (*incomplete; www links will be deleted in the final version*)

1363 Altmann R. Die Elementarorganismen und ihre Beziehungen zu den Zellen. Zweite vermehrte
1364 Auflage. Verlag Von Veit & Comp, Leipzig 1894;160 pp. -

1365 www.mitoeagle.org/index.php/Altmann_1894_Verlag_Von_Veit_%26_Comp

- 1366 Birkedal R, Laasmaa M, Vendelin M. The location of energetic compartments affects
1367 energetic communication in cardiomyocytes. *Front Physiol* 2014;5:376. doi:
1368 10.3389/fphys.2014.00376. eCollection 2014. PMID: 25324784
- 1369 Breton S, Beaupré HD, Stewart DT, Hoeh WR, Blier PU. The unusual system of doubly
1370 uniparental inheritance of mtDNA: isn't one enough? *Trends Genet* 2007;23:465-74.
- 1371 Brown GC. Control of respiration and ATP synthesis in mammalian mitochondria and cells.
1372 *Biochem J* 1992;284:1-13. - www.mitoeagle.org/index.php/Brown_1992_Biochem_J
- 1373 Campos JC, Queliconi BB, Bozi LHM, Bechara LRG, Dourado PMM, Andres AM, Jannig
1374 PR, Gomes KMS, Zambelli VO, Rocha-Resende C, Guatimosim S, Brum PC, Mochly-
1375 Rosen D, Gottlieb RA, Kowaltowski AJ, Ferreira JCB. Exercise reestablishes
1376 autophagic flux and mitochondrial quality control in heart failure. *Autophagy*
1377 2017;13:1304-317.
- 1378 Chance B, Williams GR. Respiratory enzymes in oxidative phosphorylation. I. Kinetics of
1379 oxygen utilization. *J Biol Chem* 1955a;217:383-93. -
1380 http://www.mitoeagle.org/index.php/Chance_1955_J_Biol_Chem-I
- 1381 Chance B, Williams GR. Respiratory enzymes in oxidative phosphorylation: III. The steady
1382 state. *J Biol Chem* 1955b;217:409-27. -
1383 www.mitoeagle.org/index.php/Chance_1955_J_Biol_Chem-III
- 1384 Chance B, Williams GR. Respiratory enzymes in oxidative phosphorylation. IV. The
1385 respiratory chain. *J Biol Chem* 1955c;217:429-38. -
1386 www.mitoeagle.org/index.php/Chance_1955_J_Biol_Chem-IV
- 1387 Chance B, Williams GR. The respiratory chain and oxidative phosphorylation. *Adv Enzymol*
1388 *Relat Subj Biochem* 1956;17:65-134. -
1389 www.mitoeagle.org/index.php/Chance_1956_Adv_Enzymol_Relat_Subj_Biochem
- 1390 Cobb LJ, Lee C, Xiao J, Yen K, Wong RG, Nakamura HK, Mehta HH, Gao Q, Ashur C,
1391 Huffman DM, Wan J, Muzumdar R, Barzilai N, Cohen P. Naturally occurring

- 1392 mitochondrial-derived peptides are age-dependent regulators of apoptosis, insulin
1393 sensitivity, and inflammatory markers. *Aging* (Albany NY) 2016;8:796-809.
- 1394 Cohen ER, Cvitas T, Frey JG, Holmström B, Kuchitsu K, Marquardt R, Mills I, Pavese F,
1395 Quack M, Stohner J, Strauss HL, Takami M, Thor HL. Quantities, units and symbols in
1396 physical chemistry, IUPAC Green Book 2008;3rd Edition, 2nd Printing, IUPAC & RSC
1397 Publishing, Cambridge. -
1398 www.mitoeagle.org/index.php/Cohen_2008_IUPAC_Green_Book
- 1399 Cooper H, Hedges LV, Valentine JC (eds). The handbook of research synthesis and meta-
1400 analysis. Russell Sage Foundation 2009.
- 1401 Coopersmith J. Energy, the subtle concept. The discovery of Feynman's blocks from Leibnitz
1402 to Einstein. Oxford University Press 2010;400 pp.
- 1403 Cummins J. Mitochondrial DNA in mammalian reproduction. *Rev Reprod* 1998;3:172–82.
- 1404 Dai Q, Shah AA, Garde RV, Yonish BA, Zhang L, Medvitz NA, Miller SE, Hansen EL, Dunn
1405 CN, Price TM. A truncated progesterone receptor (PR-M) localizes to the
1406 mitochondrion and controls cellular respiration. *Mol Endocrinol* 2013;27:741-53.
- 1407 Duarte FV, Palmeira CM, Rolo AP. The role of microRNAs in mitochondria: small players
1408 acting wide. *Genes* (Basel) 2014;5:865-86.
- 1409 Dufour S, Rousse N, Canioni P, Diolez P. Top-down control analysis of temperature effect on
1410 oxidative phosphorylation. *Biochem J* 1996;314:743-51.
- 1411 Ernster L, Schatz G Mitochondria: a historical review. *J Cell Biol* 1981;91:227s-55s. -
1412 www.mitoeagle.org/index.php/Ernster_1981_J_Cell_Biol
- 1413 Estabrook RW. Mitochondrial respiratory control and the polarographic measurement of
1414 ADP:O ratios. *Methods Enzymol* 1967;10:41-7. -
1415 www.mitoeagle.org/index.php/Estabrook_1967_Methods_Enzymol
- 1416 Faber C, Zhu ZJ, Castellino S, Wagner DS, Brown RH, Peterson RA, Gates L, Barton J,
1417 Bickett M, Hagerty L, Kimbrough C, Sola M, Bailey D, Jordan H, Elangbam CS.

- 1418 Cardiolipin profiles as a potential biomarker of mitochondrial health in diet-induced
1419 obese mice subjected to exercise, diet-restriction and ephedrine treatment. *J Appl*
1420 *Toxicol* 2014;34:1122-9.
- 1421 Fell D. *Understanding the control of metabolism*. Portland Press 1997.
- 1422 Garlid KD, Semrad C, Zinchenko V. Does redox slip contribute significantly to mitochondrial
1423 respiration? In: Schuster S, Rigoulet M, Ouhabi R, Mazat J-P (eds) *Modern trends in*
1424 *biothermokinetics*. Plenum Press, New York, London 1993;287-93.
- 1425 Gerö D, Szabo C. Glucocorticoids suppress mitochondrial oxidant production via
1426 upregulation of uncoupling protein 2 in hyperglycemic endothelial cells. *PLoS One*
1427 2016;11:e0154813.
- 1428 Gnaiger E. Efficiency and power strategies under hypoxia. Is low efficiency at high glycolytic
1429 ATP production a paradox? In: *Surviving Hypoxia: Mechanisms of Control and*
1430 *Adaptation*. Hochachka PW, Lutz PL, Sick T, Rosenthal M, Van den Thillart G (eds.)
1431 CRC Press, Boca Raton, Ann Arbor, London, Tokyo 1993a:77-109. -
1432 www.mitoeagle.org/index.php/Gnaiger_1993_Hypoxia
- 1433 Gnaiger E. Nonequilibrium thermodynamics of energy transformations. *Pure Appl Chem*
1434 1993b;65:1983-2002. - www.mitoeagle.org/index.php/Gnaiger_1993_Pure_Appl_Chem
- 1435 Gnaiger E. Bioenergetics at low oxygen: dependence of respiration and phosphorylation on
1436 oxygen and adenosine diphosphate supply. *Respir Physiol* 2001;128:277-97. -
1437 www.mitoeagle.org/index.php/Gnaiger_2001_Respir_Physiol
- 1438 Gnaiger E. *Mitochondrial pathways and respiratory control. An introduction to OXPHOS*
1439 *analysis*. 4th ed. *Mitochondr Physiol Network* 2014;19.12. Oroboros MiPNet
1440 Publications, Innsbruck:80 pp. -
1441 www.mitoeagle.org/index.php/Gnaiger_2014_MitoPathways

- 1442 Gnaiger E. Capacity of oxidative phosphorylation in human skeletal muscle. New
1443 perspectives of mitochondrial physiology. *Int J Biochem Cell Biol* 2009;41:1837-45. -
1444 www.mitoeagle.org/index.php/Gnaiger_2009_Int_J_Biochem_Cell_Biol
- 1445 Gnaiger E, Méndez G, Hand SC. High phosphorylation efficiency and depression of
1446 uncoupled respiration in mitochondria under hypoxia. *Proc Natl Acad Sci USA*
1447 2000;97:11080-5. -
1448 www.mitoeagle.org/index.php/Gnaiger_2000_Proc_Natl_Acad_Sci_U_S_A
- 1449 Greggio C, Jha P, Kulkarni SS, Lagarrigue S, Broskey NT, Boutant M, Wang X, Conde
1450 Alonso S, Ofori E, Auwerx J, Cantó C, Amati F. Enhanced respiratory chain
1451 supercomplex formation in response to exercise in human skeletal muscle. *Cell Metab*
1452 2017;25:301-11. - http://www.mitoeagle.org/index.php/Greggio_2017_Cell_Metab
- 1453 Hofstadter DR. Gödel, Escher, Bach: An eternal golden braid. A metaphorical fugue on minds
1454 and machines in the spirit of Lewis Carroll. Harvester Press 1979;499 pp. -
1455 www.mitoeagle.org/index.php/Hofstadter_1979_Harvester_Press
- 1456 Illaste A, Laasmaa M, Peterson P, Vendelin M. Analysis of molecular movement reveals
1457 latticelike obstructions to diffusion in heart muscle cells. *Biophys J* 2012;102:739-48. -
1458 PMID: 22385844
- 1459 Jasienski M, Bazzaz FA. The fallacy of ratios and the testability of models in biology. *Oikos*
1460 1999;84:321-26.
- 1461 Jephthina N, Beraud N, Sepp M, Birkedal R, Vendelin M. Permeabilized rat cardiomyocyte
1462 response demonstrates intracellular origin of diffusion obstacles. *Biophys J*
1463 2011;101:2112-21. - PMID: 22067148
- 1464 Klepinin A, Ounpuu L, Guzun R, Chekulayev V, Timohhina N, Tepp K, Shevchuk I,
1465 Schlattner U, Kaambre T. Simple oxygraphic analysis for the presence of adenylate
1466 kinase 1 and 2 in normal and tumor cells. *J Bioenerg Biomembr* 2016;48:531-48. -
1467 http://www.mitoeagle.org/index.php/Klepinin_2016_J_Bioenerg_Biomembr

- 1468 Klingenberg M. UCP1 - A sophisticated energy valve. *Biochimie* 2017;134:19-27
- 1469 Koit A, Shevchuk I, Ounpuu L, Klepinin A, Chekulayev V, Timohhina N, Tepp K, Puurand
1470 M, Truu L, Heck K, Valvere V, Guzun R, Kaambre T. Mitochondrial respiration in
1471 human colorectal and breast cancer clinical material is regulated differently. *Oxid Med*
1472 *Cell Longev* 2017;1372640. -
1473 http://www.mitoeagle.org/index.php/Koit_2017_Oxid_Med_Cell_Longev
- 1474 Komlódi T, Tretter L. Methylene blue stimulates substrate-level phosphorylation catalysed by
1475 succinyl-CoA ligase in the citric acid cycle. *Neuropharmacology* 2017;123:287-98. -
1476 www.mitoeagle.org/index.php/Komlodi_2017_Neuropharmacology
- 1477 Lane N. Power, sex, suicide: Mitochondria and the meaning of life. Oxford University Press
1478 2005;354 pp.
- 1479 Larsen S, Nielsen J, Neigaard Nielsen C, Nielsen LB, Wibrand F, Stride N, Schroder HD,
1480 Boushel RC, Helge JW, Dela F, Hey-Mogensen M. Biomarkers of mitochondrial
1481 content in skeletal muscle of healthy young human subjects. *J Physiol* 590;2012:3349-
1482 60. - http://www.mitoeagle.org/index.php/Larsen_2012_J_Physiol
- 1483 Lee C, Zeng J, Drew BG, Sallam T, Martin-Montalvo A, Wan J, Kim SJ, Mehta H, Hevener
1484 AL, de Cabo R, Cohen P. The mitochondrial-derived peptide MOTS-c promotes
1485 metabolic homeostasis and reduces obesity and insulin resistance. *Cell Metab*
1486 2015;21:443-54.
- 1487 Lee SR, Kim HK, Song IS, Youm J, Dizon LA, Jeong SH, Ko TH, Heo HJ, Ko KS, Rhee BD,
1488 Kim N, Han J. Glucocorticoids and their receptors: insights into specific roles in
1489 mitochondria. *Prog Biophys Mol Biol* 2013;112:44-54.
- 1490 Leek BT, Mudaliar SR, Henry R, Mathieu-Costello O, Richardson RS. Effect of acute
1491 exercise on citrate synthase activity in untrained and trained human skeletal muscle. *Am*
1492 *J Physiol Regul Integr Comp Physiol* 2001;280:R441-7.

- 1493 Lemieux H, Blier PU, Gnaiger E. Remodeling pathway control of mitochondrial respiratory
1494 capacity by temperature in mouse heart: electron flow through the Q-junction in
1495 permeabilized fibers. *Sci Rep* 2017;7:2840. -
1496 www.mitoeagle.org/index.php/Lemieux_2017_Sci_Rep
- 1497 Lenaz G, Tioli G, Falasca AI, Genova ML. Respiratory supercomplexes in mitochondria. In:
1498 Mechanisms of primary energy trasduction in biology. M Wikstrom (ed) Royal Society
1499 of Chemistry Publishing, London, UK 2017:296-337 (in press)
- 1500 Margulis L. Origin of eukaryotic cells. New Haven: Yale University Press 1970.
- 1501 Meinild Lundby AK, Jacobs RA, Gehrig S, de Leur J, Hauser M, Bonne TC, Flück D,
1502 Dandanell S, Kirk N, Kaech A, Ziegler U, Larsen S, Lundby C. Exercise training
1503 increases skeletal muscle mitochondrial volume density by enlargement of existing
1504 mitochondria and not de novo biogenesis. *Acta Physiol (Oxf)* 2017;[Epub ahead of
1505 print].
- 1506 Menshikova EV, Ritov VB, Fairfull L, Ferrell RE, Kelley DE, Goodpaster BH. Effects of
1507 exercise on mitochondrial content and function in aging human skeletal muscle. *J*
1508 *Gerontol A Biol Sci Med Sci* 2006;61:534-40.
- 1509 Menshikova EV, Ritov VB, Ferrell RE, Azuma K, Goodpaster BH, Kelley DE.
1510 Characteristics of skeletal muscle mitochondrial biogenesis induced by moderate-
1511 intensity exercise and weight loss in obesity. *J Appl Physiol (1985)* 2007;103:21-7.
- 1512 Menshikova EV, Ritov VB, Toledo FG, Ferrell RE, Goodpaster BH, Kelley DE. Effects of
1513 weight loss and physical activity on skeletal muscle mitochondrial function in obesity.
1514 *Am J Physiol Endocrinol Metab* 2005;288:E818-25.
- 1515 Miller GA. The science of words. Scientific American Library New York 1991;276 pp. -
1516 www.mitoeagle.org/index.php/Miller_1991_Scientific_American_Library

- 1517 Mitchell P. Chemiosmotic coupling in oxidative and photosynthetic phosphorylation *Biochim*
1518 *Biophys Acta Bioenergetics* 2011;1807:1507-38. -
1519 <http://www.sciencedirect.com/science/article/pii/S0005272811002283>
- 1520 Mitchell P, Moyle J. Respiration-driven proton translocation in rat liver mitochondria.
1521 *Biochem J* 1967;105:1147-62. -
1522 www.mitoeagle.org/index.php/Mitchell_1967_Biochem_J
- 1523 Mogensen M, Sahlin K, Fernström M, Glinborg D, Vind BF, Beck-Nielsen H, Højlund K.
1524 Mitochondrial respiration is decreased in skeletal muscle of patients with type 2
1525 diabetes. *Diabetes* 2007;56:1592-9.
- 1526 Moreno M, Giacco A, Di Munno C, Goglia F. Direct and rapid effects of 3,5-diiodo-L-
1527 thyronine (T2). *Mol Cell Endocrinol* 2017;7207:30092-8.
- 1528 Morrow RM, Picard M, Derbeneva O, Leipzig J, McManus MJ, Gouspillou G, Barbat-Artigas
1529 S, Dos Santos C, Hepple RT, Murdock DG, Wallace DC. Mitochondrial energy
1530 deficiency leads to hyperproliferation of skeletal muscle mitochondria and enhanced
1531 insulin sensitivity. *Proc Natl Acad Sci U S A* 2017;114:2705-10. -
1532 www.mitoeagle.org/index.php/Morrow_2017_Proc_Natl_Acad_Sci_U_S_A
- 1533 Nicholls DG, Ferguson S. *Bioenergetics 4*. Elsevier 2013.
- 1534 Paradies G, Paradies V, De Benedictis V, Ruggiero FM, Petrosillo G. Functional role of
1535 cardiolipin in mitochondrial bioenergetics. *Biochim Biophys Acta* 2014;1837:408-17. -
1536 http://www.mitoeagle.org/index.php/Paradies_2014_Biochim_Biophys_Acta
- 1537 Pesta D, Hoppel F, Macek C, Messner H, Faulhaber M, Kobel C, Parson W, Burtscher M,
1538 Schocke M, Gnaiger E. Similar qualitative and quantitative changes of mitochondrial
1539 respiration following strength and endurance training in normoxia and hypoxia in
1540 sedentary humans. *Am J Physiol Regul Integr Comp Physiol* 2011;301:R1078-87.
- 1541 Price TM, Dai Q. The Role of a Mitochondrial Progesterone Receptor (PR-M) in
1542 Progesterone Action. *Semin Reprod Med.* 2015;33:185-94.

- 1543 Prigogine I. Introduction to thermodynamics of irreversible processes. Interscience, New
1544 York, 1967;3rd ed.
- 1545 Puchowicz MA, Varnes ME, Cohen BH, Friedman NR, Kerr DS, Hoppel CL. Oxidative
1546 phosphorylation analysis: assessing the integrated functional activity of human skeletal
1547 muscle mitochondria – case studies. *Mitochondrion* 2004;4:377-85. -
1548 www.mitoeagle.org/index.php/Puchowicz_2004_Mitochondrion
- 1549 Puntschart A, Claassen H, Jostarndt K, Hoppeler H, Billeter R. mRNAs of enzymes involved
1550 in energy metabolism and mtDNA are increased in endurance-trained athletes. *Am J*
1551 *Physiol* 1995;269:C619-25.
- 1552 Quiros PM, Mottis A, Auwerx J. Mitonuclear communication in homeostasis and stress. *Nat*
1553 *Rev Mol Cell Biol* 2016;17:213-26.
- 1554 Reichmann H, Hoppeler H, Mathieu-Costello O, von Bergen F, Pette D. Biochemical and
1555 ultrastructural changes of skeletal muscle mitochondria after chronic electrical
1556 stimulation in rabbits. *Pflugers Arch* 1985;404:1-9.
- 1557 Renner K, Amberger A, Konwalinka G, Gnaiger E. Changes of mitochondrial respiration,
1558 mitochondrial content and cell size after induction of apoptosis in leukemia cells.
1559 *Biochim Biophys Acta* 2003;1642:115-23. -
1560 www.mitoeagle.org/index.php/Renner_2003_Biochim_Biophys_Acta
- 1561 Rich P. Chemiosmotic coupling: The cost of living. *Nature* 2003;421:583. -
1562 www.mitoeagle.org/index.php/Rich_2003_Nature
- 1563 Rostovtseva TK, Sheldon KL, Hassanzadeh E, Monge C, Saks V, Bezrukov SM, Sackett DL.
1564 Tubulin binding blocks mitochondrial voltage-dependent anion channel and regulates
1565 respiration. *Proc Natl Acad Sci USA* 2008;105:18746-51. -
1566 www.mitoeagle.org/index.php/Rostovtseva_2008_Proc_Natl_Acad_Sci_U_S_A

- 1567 Rustin P, Parfait B, Chretien D, Bourgeron T, Djouadi F, Bastin J, Rötig A, Munnich A.
1568 Fluxes of nicotinamide adenine dinucleotides through mitochondrial membranes in
1569 human cultured cells. *J Biol Chem* 1996;271:14785-90.
- 1570 Saks VA, Veksler VI, Kuznetsov AV, Kay L, Sikk P, Tiivel T, Tranqui L, Olivares J, Winkler
1571 K, Wiedemann F, Kunz WS. Permeabilised cell and skinned fiber techniques in studies
1572 of mitochondrial function in vivo. *Mol Cell Biochem* 1998;184:81-100. -
1573 http://www.mitoeagle.org/index.php/Saks_1998_Mol_Cell_Biochem
- 1574 Salabei JK, Gibb AA, Hill BG. Comprehensive measurement of respiratory activity in
1575 permeabilized cells using extracellular flux analysis. *Nat Protoc* 2014;9:421-38.
- 1576 Sazanov LA. A giant molecular proton pump: structure and mechanism of respiratory
1577 complex I. *Nat Rev Mol Cell Biol* 2015;16:375-88. -
1578 www.mitoeagle.org/index.php/Sazanov_2015_Nat_Rev_Mol_Cell_Biol
- 1579 Schneider TD. Claude Shannon: biologist. The founder of information theory used biology to
1580 formulate the channel capacity. *IEEE Eng Med Biol Mag* 2006;25:30-3.
- 1581 Schönfeld P, Dymkowska D, Wojtczak L. Acyl-CoA-induced generation of reactive oxygen
1582 species in mitochondrial preparations is due to the presence of peroxisomes. *Free Radic*
1583 *Biol Med* 2009;47:503-9.
- 1584 Schrödinger E. *What is life? The physical aspect of the living cell.* Cambridge Univ Press,
1585 1944. - www.mitoeagle.org/index.php/Gnaiger_1994_BTK
- 1586 Schultz J, Wiesner RJ. Proliferation of mitochondria in chronically stimulated rabbit skeletal
1587 muscle--transcription of mitochondrial genes and copy number of mitochondrial DNA.
1588 *J Bioenerg Biomembr* 2000;32:627-34.
- 1589 Simson P, Jepihhina N, Laasmaa M, Peterson P, Birkedal R, Vendelin M. Restricted ADP
1590 movement in cardiomyocytes: Cytosolic diffusion obstacles are complemented with a
1591 small number of open mitochondrial voltage-dependent anion channels. *J Mol Cell*
1592 *Cardiol* 2016;97:197-203. - PMID: 27261153

- 1593 Stucki JW, Ineichen EA. Energy dissipation by calcium recycling and the efficiency of
1594 calcium transport in rat-liver mitochondria. *Eur J Biochem* 1974;48:365-75.
- 1595 Tonkonogi M, Harris B, Sahlin K. Increased activity of citrate synthase in human skeletal
1596 muscle after a single bout of prolonged exercise. *Acta Physiol Scand* 1997;161:435-6.
- 1597 Waczulikova I, Habodaszova D, Cagalinec M, Ferko M, Ulicna O, Mateasik A, Sikurova L,
1598 Ziegelhöffer A. Mitochondrial membrane fluidity, potential, and calcium transients in
1599 the myocardium from acute diabetic rats. *Can J Physiol Pharmacol* 2007;85:372-81.
- 1600 Wagner BA, Venkataraman S, Buettner GR. The rate of oxygen utilization by cells. *Free*
1601 *Radic Biol Med.* 2011;51:700-712.
1602 <http://dx.doi.org/10.1016/j.freeradbiomed.2011.05.024> PMID: PMC3147247
- 1603 Wang H, Hiatt WR, Barstow TJ, Brass EP. Relationships between muscle mitochondrial
1604 DNA content, mitochondrial enzyme activity and oxidative capacity in man: alterations
1605 with disease. *Eur J Appl Physiol Occup Physiol* 1999;80:22-7.
- 1606 Watt IN, Montgomery MG, Runswick MJ, Leslie AG, Walker JE. Bioenergetic cost of
1607 making an adenosine triphosphate molecule in animal mitochondria. *Proc Natl Acad Sci*
1608 *U S A* 2010;107:16823-7. -
1609 www.mitoeagle.org/index.php/Watt_2010_Proc_Natl_Acad_Sci_U_S_A
- 1610 Weibel ER, Hoppeler H. Exercise-induced maximal metabolic rate scales with muscle aerobic
1611 capacity. *J Exp Biol* 2005;208:1635-44.
- 1612 White DJ, Wolff JN, Pierson M, Gemmell NJ. Revealing the hidden complexities of mtDNA
1613 inheritance. *Mol Ecol* 17; 2008:4925-42.
- 1614 Wikström M, Hummer G. Stoichiometry of proton translocation by respiratory complex I and
1615 its mechanistic implications. *Proc Natl Acad Sci U S A* 2012;109:4431-6. -
1616 www.mitoeagle.org/index.php/Wikstroem_2012_Proc_Natl_Acad_Sci_U_S_A
- 1617 Willis WT, Jackman MR, Messer JJ, Kuzmiak-Glancy S, Glancy B. A simple hydraulic
1618 analog model of oxidative phosphorylation. *Med Sci Sports Exerc.* 2016;48:990-1000.